



Satellite Altimetry Measurements of Sea Level in the Coastal Zone

Stefano Vignudelli¹ · Florence Birol² · Jérôme Benveniste³ · Lee-Lueng Fu⁴ · Nicolas Picot⁵ · Matthias Raynal⁶ · H el ene Roinard⁶

Received: 4 December 2018 / Accepted: 13 August 2019 / Published online: 16 October 2019
  Springer Nature B.V. 2019

Abstract

Satellite radar altimetry provides a unique sea level data set that extends over more than 25 years back in time and that has an almost global coverage. However, when approaching the coasts, the extraction of correct sea level estimates is challenging due to corrupted waveforms and to errors in most of the corrections and in some auxiliary information used in the data processing. The development of methods dedicated to the improvement of altimeter data in the coastal zone dates back to the 1990s, but the major progress happened during the last decade thanks to progress in radar technology [e.g., synthetic aperture radar (SAR) mode and Ka-band frequency], improved waveform retracking algorithms, the availability of new/improved corrections (e.g., wet troposphere and tidal models) and processing workflows oriented to the coastal zone. Today, a set of techniques exists for the processing of coastal altimetry data, generally called “coastal altimetry.” They have been used to generate coastal altimetry products. Altimetry is now recognized as part of the integrated observing system devoted to coastal sea level monitoring. In this article, we review the recent technical advances in processing and the new technological capabilities of satellite radar altimetry in the coastal zone. We also illustrate the fast-growing use of coastal altimetry data sets in coastal sea level research and applications, as high-frequency (tides and storm surge) and long-term sea level change studies.

Keywords Sea level · Coastal zone · Satellite altimetry

1 Introduction

Monitoring the coastal ocean is of first importance since changes in its environmental conditions may affect about 40% of the world’s population that lives within 100 km of the coast (Kummu et al. 2016) and that, in the future, is expected to rise at greater rates than inland (Neumann et al. 2015). The coastal ocean is a buffer region between the open sea and land, which is under increased pressures because of climate change, population growth and expanding economic development (Halpern et al. 2015). The coastal zone also

✉ Stefano Vignudelli
vignudelli@pi.ibf.cnr.it

Extended author information available on the last page of the article

faces unique risks from storm surge events and sea level rise. The presence of land makes understanding the ocean processes in the coastal zone more difficult than in the open ocean (Wright and Nichols 2018). The typical shallower water, bathymetric gradients, shoreline shapes, outflow of rivers and estuaries make the geophysical interpretation of the retrieved radar altimeter signal much more complex and have also an effect on the auxiliary information used to derive geophysical parameters (Vignudelli et al. 2011a). Knowledge of ocean tides, ocean circulation, sea level are all important requirements for the coastal zone. In particular, the impact of sea level is especially sensitive at the coast. The coastal zone infrastructure and communities are developing on present sea levels, and understanding how sea level varies from the deep ocean to the coastline is key to forecast future changes.

Since the nineteenth century, the classical method to measure sea level changes is using tide gauges (Emery and Aubrey 1991). They are located near shore to measure sea level changes relative to land with frequent sampling at the location where they are installed (see Marcos et al. 2019). While there are numerous tide gauges along the entire worldwide coastline (Fig. 1), there is only a sparse network that has produced enough long-term time series and there are important gaps especially in developing countries or remote places where it is difficult or expensive to install instruments (Woodworth et al. 2016). Moreover, there are few tide gauges around the world exactly co-located with global navigation satellite system (GNSS) stations operating continuously to measure vertical land motion (VLM) for the whole altimetry era from 1992 to now (Woodworth et al. 2017).

A complementary technology called satellite altimetry offered a new way of measuring sea level changes from space (Fu and Cazenave 2001). It is a mature technique that has provided an accurate estimate of changes in sea level every 10 days for more than 25 years over the open ocean. There is consensus from a large community of scientists about the interpretation of the altimetric signals at various scales and the legitimacy of open-ocean sea level products (Stammer and Cazenave 2017).

Tide gauges are mainly located in protected environments, not often representative of offshore conditions. Moreover, the coastal zone is affected by several local ocean processes, all impacting sea level at different scales. This means that the spatial and temporal

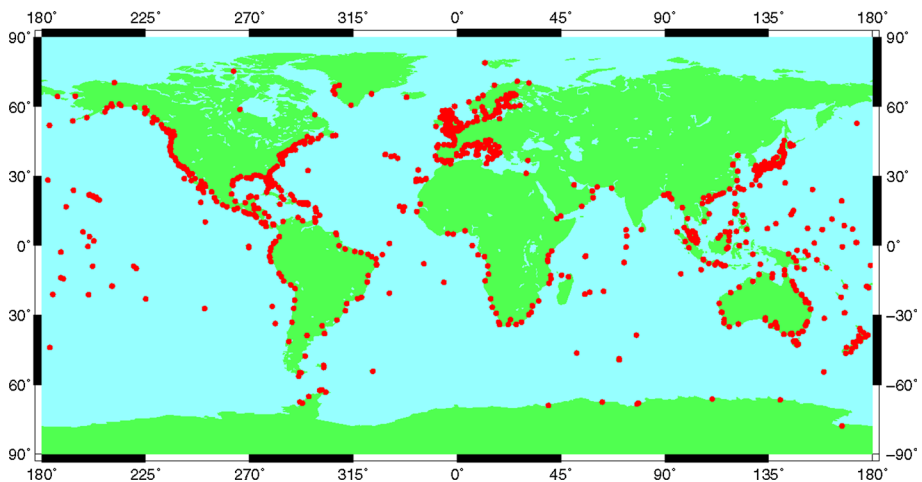


Fig. 1 Map of tide gauge stations with water surface elevations in the Global Extreme Sea Level Analysis (GESLA-2) dataset. Data from Woodworth et al. (2017)

complexity of coastal sea level is difficult to represent with only sparse tide gauges (Roemich et al. 2017). Satellite altimetry would provide a unique and consistent data set from the open ocean up to the coasts. However, traditionally, data from standard products in the coastal zone (roughly 30 km from the coast) were not processed in this region and therefore flagged as bad and left unused. Therefore, traditional altimetry retrievals were unable to produce meaningful signals of sea level change in the coastal zone (Vignudelli et al. 2006).

This has motivated the development of coastal altimetry to improve the data quality closer to the coast with better spatial resolution, in order to extend the satellite-based sea level record toward the coast with quality comparable to that of the open ocean (Vignudelli et al. 2011a). Moreover, progress was made in technology, with new radar techniques, e.g., synthetic aperture radar (SAR) mode also called delay/Doppler altimeter (DDA) on Cryo-Sat-2, Sentinel-3A and Sentinel-3B operating in Ku-band, and new experimental missions, e.g., the SARAL/AltiKa mission, operating in a conventional, or low-resolution model (LRM), but in Ka-band altimetry to become more capable close to the coast, opened new possibilities to better describe coastal ocean phenomena with high dynamics at fine spatial scales (Cipollini et al. 2017a, b). Therefore, coastal altimetry has the potential to deliver a unique and consistent sea level data set from the open ocean up to the coasts, which can be coupled with tide gauges and other observational techniques to improve the ability to understand coastal sea level changes (Marcos et al. 2019). Coastal altimetry can also measure changes in sea level in regions lacking in situ infrastructure.

The aim of this paper is to review the main issues when retrieving altimeter data (range and corrections) in the coastal zone and the associated techniques to get more and better data closer to the coastline. The paper also identifies the new observing capabilities of modern altimetry, new and improved data streams and products, with the ultimate aim of supporting coastal sea level research studies that are particularly important in the coastal zones subject to inundation, to understand actual conditions, determine rates of change and make reliable forecasting.

2 Satellite Altimetry and Issues in the Coastal Zone

Satellite altimetry has been originally designed for the open ocean, and the spatial and temporal resolution of sensors was supposed not to be high enough to get accurate sea levels in the coastal zone. Altimeter data require a complex sequence of processing steps to get usable information. The satellite altimetry system is based on a radar altimeter sending/receiving pulses/echoes toward/from the mean reflected surface. Over open ocean, the received echoes (called waveform) for classical altimetry follow a standard shape, with steeply rising leading edge followed by a trailing edge with gradually diminishing power. This standard shape is in agreement with the theoretical Brown model (Brown 1977) and hence can be modeled to estimate the signal round-trip time between the radar and the sea surface (Gómez-Enri et al. 2009). From this time value, a range (i.e., the distance between the satellite's center of mass and the mean reflected surface) can be determined. The recipe to transform the altimeter range into sea surface height (SSH) and sea level anomaly (SLA) also requires knowledge of auxiliary information [e.g., satellite altitude; atmospheric and sea surface corrections; mean sea surface (MSS)].

Radar altimetry waveforms can be distorted by any inhomogeneity in the properties of the surface observed (e.g., in altimeter footprints, Gómez-Enri et al. 2010). It is the case in land–ocean transition areas (e.g., Abileah et al. 2013). Ignoring these effects leads to severe

errors in the range computation. In coastal areas, waveform retracking algorithms must be able to analyze these distorted waveforms. Moreover, algorithms for various corrections must be considered (Andersen and Scharroo 2011), together with accurate orbits. It is well known that standard altimetry corrections might have reduced the accuracy in the coastal zone for two principal reasons: direct influence of land on the measurement system; reduction in scale, temporal and spatial, of both oceanographic and atmospheric processes in the coastal zone.

The atmospheric-related effects induce a delay in the electromagnetic pulse travel time, which is taken into account through the ionospheric and the tropospheric (dry and wet) corrections (Fernandes et al. 2013). The water vapor correction (known as “wet tropospheric” correction, WTC) is one of the sources of error (Desportes et al. 2007). Strong near-coast gradients in water vapor produce changes in path delay equivalent to several centimeters that must be corrected, but the open-ocean correction based on microwave radiometers is unusable closer than 20–50 km as land enters the radiometer footprint (Vieira et al. 2018).

It has been shown that the dry tropospheric correction (DTC) has strong height dependence (Fernandes et al. 2014). The DTC has a mean variation of -2.5 cm per each 100 m (Cipollini et al. 2017a, b). The DTC for most of the satellite radar altimetry missions, except for, e.g., Sentinel-3A, is interpolated in time and space from values provided at the level of the smoothed representation of the terrain of the adopted model (Cipollini et al. 2017a, b).

The sea state and wind induce effects that must be corrected: radar signals are better reflected from troughs than crests (electromagnetic bias), the median sea level is not the mean sea level (skewness bias) and the range retrieval might be biased (tracker bias); all these are combined into the sea state bias (SSB) correction. The SSB is currently one of the range corrections with the largest uncertainty in the coastal zone (Pires et al. 2016, 2018).

We also need to remove oceanographic signals whose temporal periods are not resolved by altimetry in order to avoid important aliasing errors: tides and the high frequency response to wind and pressure changes. Large errors in tidal modeling still exist in the coastal zone (Ray and Egbert 2017); therefore, subtracting this signal remains a problem (Ray et al. 2011), as tidal range in coastal regions is larger than in open ocean and more complex due to various causes (e.g., bottom friction and resonance). Moreover, the signal has much higher frequency than the sampling of the satellite. Coastal tidal models are improving, but these also require detailed bathymetric data (Toublanc et al. 2018).

The dynamic atmospheric correction (known as DAC, i.e., combining the high-frequency barotropic sea level elevations and the low-frequency sea level elevations from the inverted barometer law) is also usually applied to the altimeter range (Carrère and Lyard 2003). The performances of global models used to estimate DAC in open ocean depend on forcing weather fields and bathymetry that are not at the required resolution and accuracy for the typical variability scales of the coastal zone (Carrère et al. 2016).

Other issues must also be addressed to optimize satellite altimetry in the coastal regions including the use of the MSS (Andersen and Scharroo 2011), which is computed as a spatial and temporal average of the along-track altimetric SSH measurements (Pujol et al. 2018). Typical approaches make use of interpolation and prediction techniques, as, for instance, least squares collocation (Hwang et al. 2002). Moreover, altimeter standard data are often missing in the coastal band from the coastline to 50 km offshore; therefore, the resolution of MSS products derived from altimetry data is degraded (Roblou et al. 2011).

From the studies mentioned above and others published in the literature, a reasonable consensus emerges on the fact that the ongoing data reprocessing efforts in the coastal

zone are crucial for coastal sea level monitoring. This reprocessing relies on preprocessing (e.g., retracking, new/improved corrections) and on post-processing of higher rate data (e.g., editing). While the waveforms at high sampling rate (20/40/80 Hz corresponding to ~350/175/85 m depending on the altimeter mission) are all included within the products delivered, as well as range, significant wave height (SWH) and sigma-0 (Backscatter coefficient) that all are available at that resolution, the geophysical corrections are provided at 1 Hz (corresponding to ~7 km), and an interpolation step has to be performed to resample these fields to the native 20/40/80 Hz rate of the altimeter measurements.

3 Coastal Altimetry: A Set of Techniques

Coastal altimetry, i.e., the extension of satellite radar altimetry into the oceanic coastal zone, is an active field of research. Standard geophysical data records (GDRs) are almost useless for coastal applications, as most of the data in the coastal zone are flagged as “bad” because they are processed with the criteria used for open-ocean altimetry (Vignudelli et al. 2011b). This impediment to the use of altimetry for understanding coastal ocean processes can, however, in most cases, be overcome by removing or mitigating unwanted effects caused by the instrument, atmosphere, ocean and land. As stated previously, until recently, these effects were not sufficiently understood in the coastal zone, but the situation is rapidly evolving thanks to intense research in this field.

Coastal altimetry has made steady progress in recent years (Restano et al. 2018; Cipollini et al. 2017a, b; Vignudelli et al. 2011a) and has become a recognized mission objective for present and future satellite altimeters (Cipollini et al. 2014). Coastal altimetry can be considered as a set of techniques aiming at retrieving more and better data closer to the coast, where land contamination and inhomogeneity of radar backscattering degrade range, SSB and WTC corrections.

The traditional coastal reprocessing for conventional altimetry follows the approach based on de-flagging over-conservative flags, ad hoc filtering-out spikes in the data or in the corrections, re-interpolating missing corrections, and other processing recipes and screening applied to 1 Hz data to retain small-scale signals (e.g., Birol et al. 2006, 2017; Roblou et al. 2011).

A second generation of coastal altimetry reprocessing uses all the improvements of the first generation but also aims at getting closer to the coast, typically up to 1–5 km. As shown previously in this case there are additional problems: land which enters the footprint of the altimeter; quasi-specular reflections from stretches of calm water (for instance from a sheltered area); steepening of the waves; short-scale variability of the surface characteristics. All these factors cause a departure of the received radar waveforms from the open-ocean “Brown” model (Brown 1977) in pulse-limited altimeters used for the estimation of the parameters. Therefore, it becomes necessary to fit alternate models to the waveforms, in other words to “retrack” the waveforms (Gómez-Enri et al. 2009).

During recent years, significant improvements have been achieved thanks to more sophisticated reprocessing that now uses robust retracking algorithms for retrieving the range from altimeter’s radar echoes. Some approaches are based on some form of classification of the waveforms depending on their shape and the use of a different functional form for the fitting of each class (e.g., Deng and Featherstone 2006; Berry et al. 2010; Yang et al. 2012). Other methods process a stack of successive waveforms to detect the signature of bright targets as proposed by Gómez-Enri et al. (2010), for the purpose of “cleaning” the

stack prior to retracking (Quarty 2010). A more recent approach is based on the partitioning of the waveform in a sub-waveform containing the leading edge, thus excluding the tail section where most artifacts due to spurious bright targets from bordering land appear (e.g., Guo et al. 2010; Yang et al. 2011; Idris and Deng 2012; Passaro et al. 2014; Roscher et al. 2017; Peng and Deng 2018). The algorithms of the various authors differ in the estimator used and the method adopted to isolate the portion of the real waveform to fit with the Brown ocean model.

Advances in the observational capabilities through delay-Doppler technology and SAR/DDA processing have brought an improved observability of the small scales (Heslop et al. 2017; Raynal et al. 2018) and higher accuracy in sea level estimations (Boy et al. 2017). A growing number of publications show that the new SAR mode from CryoSat-2 and now globally from Sentinel-3A and Sentinel-3B has been particularly beneficial in the coastal zone, by virtue of the higher along-track resolution and lower noise than conventional altimetry, when the satellite ground track is perpendicular to the coastline (e.g., Gómez-Enri et al. 2018; Dinardo et al. 2018).

In situations where the satellite is orbiting parallel to the coast, the SRAL (Sentinel-3 Ku/C SAR Radar Altimeter) ground resolution cell has a greater proportion of land coverage (Boy et al. 2017). Conventional altimetry also has a greater proportion of land coverage when near the coast, as the ground resolution cell is a circle and then a ring. The difference is that it does not matter what orientation the track has. Some preliminary studies, however, limited to specific areas of investigation, seem to show some impact of land contamination (Birgiel et al. 2018), with reduced precision across track (Cotton et al. 2016). In these situations, two approaches exist to recover more data, one removing contamination using SARin mode (applicable to CryoSat-2 only) and constructing the waveform only from the remaining part (García et al. 2018), and a second one focusing on the waveform to a narrow beam (called fully focused), so that contamination can be excluded (Egido and Smith 2017). Both techniques are still in their infancy but show some promising results. The SAR mode can be processed simply unfocused up to 80 Hz, and a higher rate can be achieved with the fully focused approach.

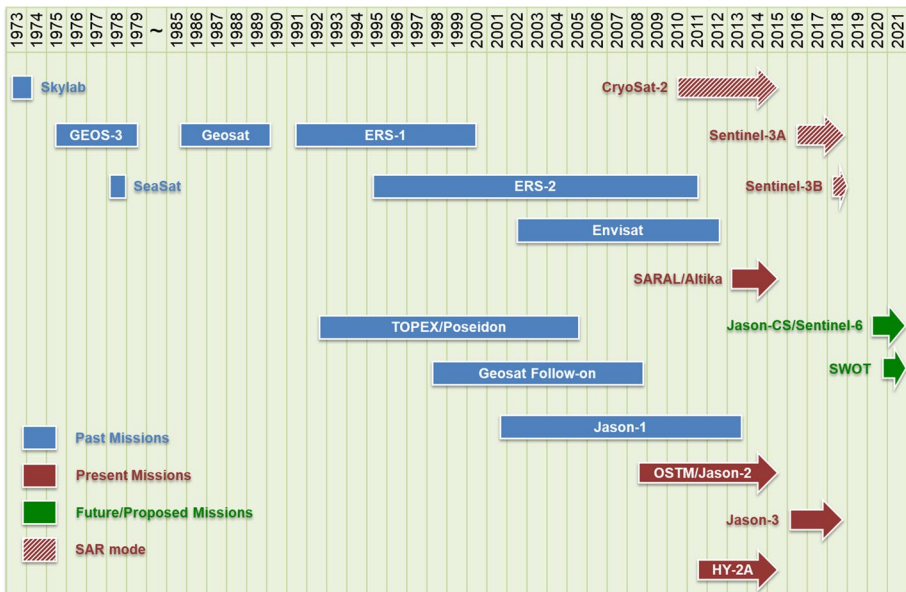
Following the successful launch in February 2013 of the SARAL/AltiKa, the first Ka-band radar altimetry mission, new capabilities emerged in the coastal zone. SARAL/AltiKa takes advantage of a reduced footprint to about 100 km², compared with larger (~300 km²) footprints of conventional altimetry (e.g., Jason series) as reported in Fig. 1.17 in Stammer and Cazenave (2017). Due to the smaller footprint, the altimeter can provide better results closer to the coasts. SARAL/AltiKa has also higher spatial resolution (up to 40 Hz) than the present conventional Ku-band (up to 20 Hz), thus enabling data retrieval much closer to the coast (Bonnefond et al. 2018; Verron et al. 2018). Progress has been made in reducing the altimeter footprints and noise going closer to the coast, but also in processing algorithms, corrections, and products for coastal applications (Valladeau et al. 2015). Moreover, the higher Ka-band frequency (35 GHz vs. 13 GHz for Ku-band) permits the use of a larger bandwidth than other altimeters, thus enhancing the resolution of the waveform gates to 0.3 m (Verron et al. 2018).

Reprocessed experimental products dedicated to the monitoring of coastal sea level are now available (e.g., COASTALT, ALES, XTRACK, PISTACH, SARvatore, TUDaBo). Compared to standard products, they include higher along-track resolution, new/improved retrackers, new/improved corrections, refined preprocessing, and/or post-processing. Cipollini et al. (2017a, b) summarized the main characteristics of the available products. The above products differ for their processing approach, applied

geophysical corrections, coverage, satellite missions. An updated table is accessible at www.coastalt.eu/datasets, as algorithms and methodological approaches will continue to mature over the coming decades.

X-TRACK is a 1-Hz along-track product available in 23 regions with consistent and homogeneous coastal processing for some altimetric missions (TOPEX/Poseidon, Jason-1&2&3, Geosat Follow-on, Envisat, SARAL). However, a global 20-Hz product for all available missions is not yet available. The European Space Agency (ESA) Climate Change Initiative (CCI) project on “Sea Level” has reprocessed altimeter data from nine satellite missions over 1993–2015 to provide homogenous sea level for all altimetry missions (Legeais et al. 2018) over a grid of around 25 km, with the objective of improving estimations of climate-related sea level changes (Ablain et al. 2017) and consequently proposed a climate processing standard that has been replicated in other processing systems. The CCI+ new phase will address the last 50 km to the coast, with a coastal reprocessing for all missions and generation of a coastal altimetry product dedicated to long-term coastal sea level monitoring (Cazenave et al. 2018).

At the time of writing, there are height altimetry satellites currently in service (Jason-2, Jason-3, SARAL/AltiKa, HY2-A/B, CryoSat-2, Sentinel-3A and Sentinel-3B), plus the SWIM real-aperture Ku-band radar (Hauser et al. 2017) on board the China-France CFOSAT satellite, which also takes nadir-view altimetric measurements, and more than 25 years of data archived from previous satellite missions (Fig. 2). This multi-mission data set with coastal-oriented reprocessing applied represents an important asset to support sea level research in the coastal zone.



4 Impact of Geophysical Corrections Near the Coast

As shown previously, some of the corrections applied to the altimeter range suffer from large uncertainties in the coastal zone and/or in shallow waters (Vignudelli et al. 2005; Andersen and Scharroo 2011; Ray et al. 2011) either because they have large spatiotemporal variability that is poorly reproduced by numerical models (e.g., ocean tide and DAC corrections), or because they are less precisely estimated by onboard sensors than over the open ocean (e.g., the radiometer-based WTC that suffers severe land contamination), or even because they are deduced from the altimeter measurements impacted by the proximity of land (e.g., the ionospheric correction and the SSB). As a consequence, near coastlines, the quality of the resulting SSH data degrades as the quality of the corrections applied diminishes. A complete review on this issue can be found in Vignudelli et al. (2011a).

At a global scale, the geophysical corrections that may induce the larger errors on radar altimetry coastal sea level data are: the wet tropospheric delay, the ocean tide correction, the DAC, and the SSB (Andersen and Scharroo 2011). The radiometer-based WTC degrades rapidly in a coastal band of 10–40 km, leading to errors of a few centimeters (depending on the radiometer onboard the satellite, see Fig. 6 of Cipollini et al. 2017a, b). In Jason-2/3 missions, new dedicated algorithms are implemented to largely reduce the effects of land contamination in the radiometer footprint (Brown 2010) and the improved correction is now available in classical GDR products. This correction can also be derived from atmospheric models, but their resolution does not allow capturing the spatial and temporal short-scale changes in water vapor in the coastal zone. Other solutions consist in removing the contamination coming from the surrounding land from the radiometer measurements (Brown 2010; Obligis et al. 2011). The GNSS-derived Path Delay Plus (GPD+) correction, combining valid measurements from the onboard radiometer, from GNSS coastal and island stations and from scanning radiometers on board various remote sensing missions, is one of the most recent algorithms to retrieve improved WTC for most radar altimeter missions (Fernandes et al. 2015; Fernandes and Lázaro 2016). The operational computation of the GPD+ correction has been implemented for all altimeter missions at University of Porto (Joana Fernandes, personal communication). The use of this correction improves significantly the altimeter coastal sea level estimations and the estimation of regional sea level trends (Cipollini et al. 2017a, b).

For coastal altimetry, the availability of accurate ocean tide and DAC corrections in shallow water areas is a critical issue (Andersen and Scharroo 2011). These geophysical effects tend to be much larger, complex and associated with higher wavenumbers in coastal waters than in deep waters. Considerable efforts have already been dedicated to improve the numerical tidal solutions. Regular exercises of tidal model inter-comparisons [as in Stammer et al. (2014)] highlight that much progress has been achieved in global tidal solutions. But significant differences are still observed in some coastal areas: For the major constituents, the difference between ocean tide observations and global model solutions is larger than 5 cm on average [compared to less than 1 cm in the open ocean, Stammer et al. (2014)].

Modeling individual coastal regions offers significant progress for both the tidal and atmospherically forced high-frequency corrections (Roblou et al. 2011) and regional model corrections start to be available over some coastal areas (Maraldi et al. 2007; Pairaud et al. 2008; Le Bars et al. 2010). We expect to see further important progresses in coastal ocean tide and DAC corrections thanks to the efforts done on increasing the spatial model resolution and improving numerical schemes, data assimilation

techniques, and better knowledge of the coastal bathymetry and the coastline (which still suffer from significant errors in many coastal areas, as reported in Stammer et al. 2014). Note also that for some coastal altimetry applications (storm surges or assimilation in numerical models that simulate ocean tides), the ocean tide and DAC corrections may not be a source of errors since they do not need to be removed from the sea level estimates.

The SSB is also a major source of uncertainty in coastal altimetry. Present-day methods for correcting this bias are based on wave and wind information derived from the altimeter, using empirical formulations. The latter are regularly refined (Labroue et al. 2006; Tran et al. 2010), but they are established for the open ocean. Near the coast, where wind and wave conditions change rapidly in both space and time, the development of a dedicated algorithm is needed. Another strong limitation is due to the fact that the SSB computation is based on parameters derived from the retracking of the radar waveforms (SWH and wind). Near coastlines (10–15 km from the coast), where the waveforms are much more complex, the quality of the SSB correction degrades with the performance of the waveform retracker (Andersen and Scharroo 2011). Different studies indicate that the SSB estimation may be improved by inclusion of wave model information (Tran et al. 2006), use of retrackers adapted to coastal waveforms (Gómez-Enri et al. 2016) or more simply computation of regional empirical models (Passaro et al. 2018).

Finally, every shoreline is affected by specific geophysical processes and the correction issue may be significantly different from one coastal region to another. This is illustrated in Fig. 3, which shows the standard deviation of the SLA and of the different geophysical corrections as a function of latitude for 8 years of Jason-2 data. We consider two tracks located in two regions characterized by different ocean dynamics. The SLA has been computed using all the corrections whose statistics are shown in Fig. 3. We assume that a sudden and brief increase in standard deviation values indicates errors in the correction. Comparing the standard deviation of the SLA and of the individual corrections allows us to investigate the relative impact of errors in each time-variable correction in the sea level estimation. Note first that the typical values of the variability of the different corrective terms are approximately the same in both regions, except for the ocean tides (0–250 cm for track 239 against 6–8 cm for track 85, located in a microtidal region, i.e., where the tidal range is less than 2 m).

The corrections that have the largest variability are the DAC and the ocean tides. This stresses the importance of having accurate estimates of these geophysical signals particularly along macro-tidal coasts such as over the NW European shelf seas. The corrections that have the lowest variability appear to be the ionospheric and the DTC. Concerning WTC, the GPD+ solution is used here. The values of the corresponding standard deviation appear very stable and do not indicate any degradation of the correction quality when approaching the coast. This result confirms that the GPD+ offers a significant improvement in coastal sea level estimations compared to the model and radiometer solutions. The standard deviation of the SSB (in the range 2–6 cm) appears more variable in space and suddenly increases in the last kilometers near the coast, where the standard deviation of the SLA exhibits unrealistic variations. This behavior is expected because waveforms are degraded by the land contamination in this coastal strip, thus impacting the estimation of epoch, SWH and wind amplitude that are used to compute SSB. These results indicate that in addition to the progress expected from future tidal and DAC model solutions, the computation of the SSB correction is clearly a field where effort is needed to gain accuracy in coastal altimetry data.

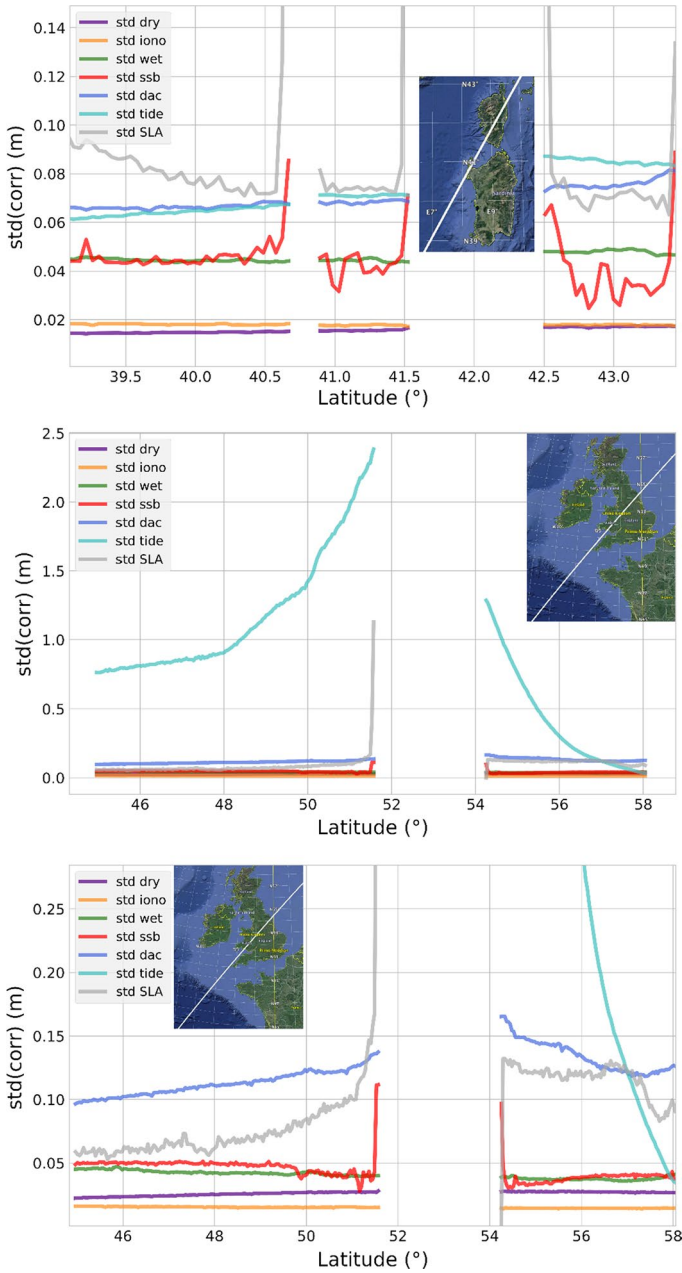


Fig. 3 Standard deviation (in meters) of the SLA and of the different geophysical corrections computed from cycles 1 to 296 of Jason-2 data along the track 85 in the Northwestern Mediterranean Sea (top) and along the track 239 in the North East Atlantic (middle and bottom). The figure at the bottom is an amplitude zoom of the figure at the middle. For each track, the region considered is indicated on the map superimposed on the figure. The corrections are derived from the RADS (Radar Altimeter Database System) database, except the wet tropospheric correction which is produced by University of Porto and distributed by the CTOH (Centre of Topography of the Oceans and the Hydrosphere)

5 Altimeter Performance Near the Coast

The onboard altimeters were initially designed to measure large-scale SSH variations in the open ocean. Their high accuracy and the large period sampled allowed improvements to our understanding of the large-scale oceanic circulation and its evolution. The extension of these observations to the coast is one of the greatest current challenges in particular for the observability of mesoscale and sub-mesoscale oceanic processes and to measure the impact of sea-level rise on our environment. However, for altimeter performances near the coasts, one of the most well-known sources of error is the footprint contamination by land surfaces. This error strongly depends on the altimeter characteristics.

Figure 4a illustrates the percentage of valid measurements computed for three different kinds of altimeter: Poseidon-3 (Jason-3), AltiKa (SARAL/AltiKa) and SRAL (Sentinel-3A), respectively, operating in LRM Ku-band, LRM Ka-band and SARM (SAR mode) Ku-band. In order to compare relevant metrics derived from the different satellites ground tracks, this statistic is computed for all ocean coastal areas over a period of 1 month. The validity criterion chosen is based on a threshold applied on SLA measurements. Indeed,

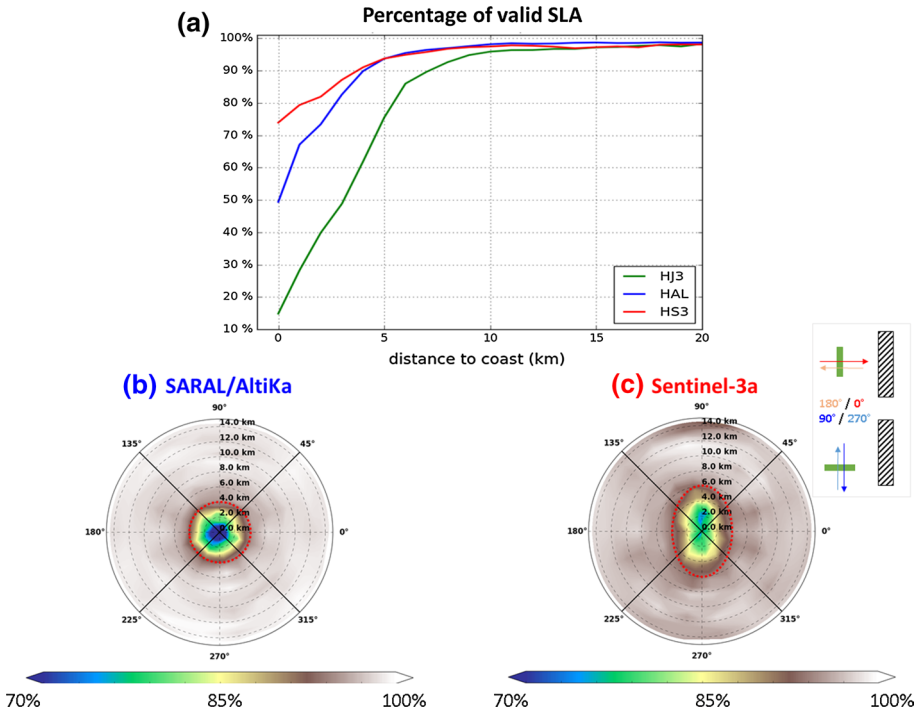


Fig. 4 Plot **a** shows the percentage of 20 Hz valid measurements computed for Sentinel-3A (red curve), SARAL/AltiKa (blue curve), and Jason-3 (green curve) datasets as a function of the distance to the coast. For this diagnosis, a measurement is considered as valid if the unbiased SLA does not exceed 1 m. Plots **b**, **c** show the percentage of valid measurements for SARAL/AltiKa and Sentinel-3A datasets (respectively, **b** and **c**). The radius of the circle corresponds to the distance of the measurement from the closest coast line. The perimeter of the circle corresponds to the angle formed between the ground track of the satellite and the closest coastline. 0° and 180° angles correspond to a perpendicular approach, whereas 90° and 270° angles correspond to parallel displacement

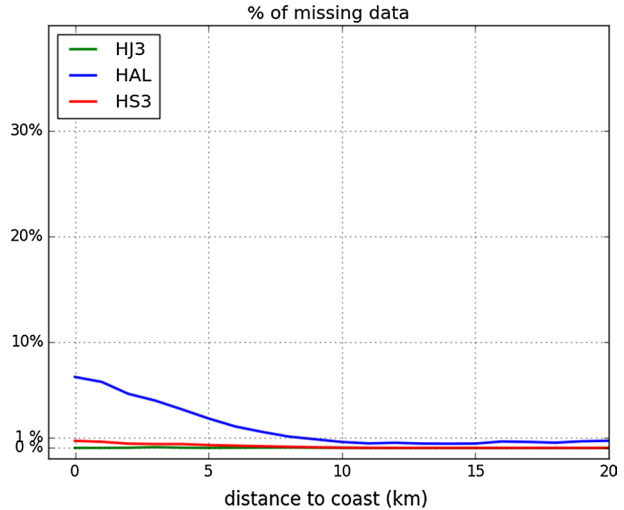
the usual 1 Hz editing provided in users handbooks is not relevant for high-rate measurements. Moreover, this choice of a 1-m threshold across the SLA mean value is a compromise for removing the strong outliers and keeping the measurements affected by the coast to illustrate the different kinds of altimeter performance (Figs. 4a, 6). The result shows a clear decrease in the number of valid measurements when the satellites approach the coast. However, the impact of the land contamination differs for the three altimeters:

- For Jason-3, the percentage of valid measurements starts to decrease around 10 km off the coast. From more than 98% in open ocean, it reaches only 15% at hundreds of meters to the coast. The value of 10 km roughly corresponds to the radius of the altimeter footprint.
- For SARAL/AltiKa, the decrease is smoother and starts around 6 km from the coast. This is explained by the smaller Ka footprint for which the radius equals 5.7 km on average. Moreover, the antenna gain pattern allows reducing the energy of the signals the farthest from the nadir (factor 2 for range gates at 4.5 km from nadir). Within 4.5 km to the coast, 50% of the measurements are still exploitable for estimating sea level.
- Finally, in the case of Sentinel-3A SARM mode dataset, the percentage of valid measurements decreases but more slightly than for other altimeters. This is explained by the specific geometry of the SARM footprint with its 300 m of resolution in the along-track direction.

The two polar plots show for SARAL/AltiKa (Fig. 4b) and Sentinel-3A (Fig. 4c) the percentage of valid SLA measurements as a function of the distance to the coast (radius of the circle) and as a function of the angle formed between the satellite ground track and the coastline (degrees of the circle). For AltiKa, as expected the direction of the satellite with respect to the coastline has no impact on the data quality (the footprint shape is circular). However, for Sentinel-3A SARM datasets an asymmetry is observed. When the satellite ground track is perpendicular to the coastline, the footprint contamination occurs much later (theoretically at 300 m from the coast). This result would mean that in these specific cases, the SARM range measurements are almost not impacted by the coast.

In addition to the altimeter signal and antenna characteristics, the tracker performances also play an important role in coastal areas. The tracker is responsible for the acquisition of the backscattered signal (Roca et al. 2009; Desjonquères et al. 2010). Two different tracking modes could be distinguished: the conventional close loop (CL) mode and (implemented for the first time on Jason-2 Poseidon-3 altimeter) the open loop (OL) mode. While in CL mode the tracker adjusts the position of the observation windows as a function of the level of energy of the backscattered signal; in OL mode an onboard predetermined digital elevation model is used. Figure 5 illustrates the altimeter tracking performances in terms of number of available measurements (with respect to the theoretical high-resolution ground track) derived from different satellites as a function of the distance to the coast. Once again, in order to compare results derived from the different satellites ground track, the diagnoses were performed over a period of 1 month including all the ocean coastal areas. Over this period, while SRAL and Poseidon-3 tracker operate in OL mode, the AltiKa tracker is in CL mode (SARAL/AltiKa geodetic phase). Despite its smaller footprint, the percentage of missing measurements for AltiKa starts to increase at 10 km from the coast, while it stays flat for Sentinel-3A. This result means that 3% (respectively, 8%) of the time, at 5 km (respectively, 0 km) from the coast, AltiKa tracker loses the signal and thus cannot provide sea surface measurements. The

Fig. 5 Percentage of 20 Hz missing measurements computed for Sentinel-3A (red curve), SARAL/AltiKa (blue curve), and Jason-3 (green curve) datasets as a function of the distance to the coast. This percentage is computed with respect to their respective high-resolution theoretical ground track



slight difference observed between Jason-3 and Sentinel-3A (around 0.6%) could be explained by the fact that, for Sentinel-3A, all the ocean coastal areas are acquired in OL mode except the Indonesian sea area. Thus over this small region, more measurements are lost by the Sentinel-3A tracker operating in CL mode.

We have just seen that the data quality and the percentage of available measurements in coastal areas depend on the altimeter characteristics. Figure 6 aims at describing the impact on the final SSH. Global statistics of mean SLA were computed for Jason-3 (a), AltiKa (b) and Sentinel-3A SARM (c) datasets. First, this analysis shows, in the case of conventional altimetry (a and b plots), that when the satellites approach the coast, the trackers lose the return signal. For Jason-3, this loss appears at 6 km from the coast with an SLA decrease of 5 cm followed by a significant increase at 4 km. For AltiKa, the same thing is observed, respectively, at 4 and 2 km. For both satellites, the waveforms are disturbed by land backscattered signal. It occurs at different distances from the coast because of the different footprint sizes. The estimated geophysical parameters are impacted since the Brown model dedicated to oceanic waveforms (Brown 1977) is not suitable to retrack this kind of artifacts. Thanks to the smaller Sentinel-3A SARM footprint in the along-track direction, these SLA variations are not observed. The SLA signal appears flat until hundreds of meters from the coast. Examining in more detail the different angle configurations (Fig. 6d), it appears that:

- in the worst case (when Sentinel-3A ground track is parallel to the coast line) the SLA behaves similarly as for conventional altimetry (black curve). From 5 to 2 km to the coast, a decrease is observed followed by an increase in the SLA.
- in the best configuration (Sentinel-3A ground track perpendicular to the coastline), the SLA slightly increases continuously until the coastline.

Although this result (the gray curve) includes the errors related to the geophysical corrections (as mentioned in the previous section), it gives a first measure of the signal we expect to observe close to the coast when the altimeter footprint is not corrupted by land surfaces. The use of high-accuracy regional models combined with the exploitation

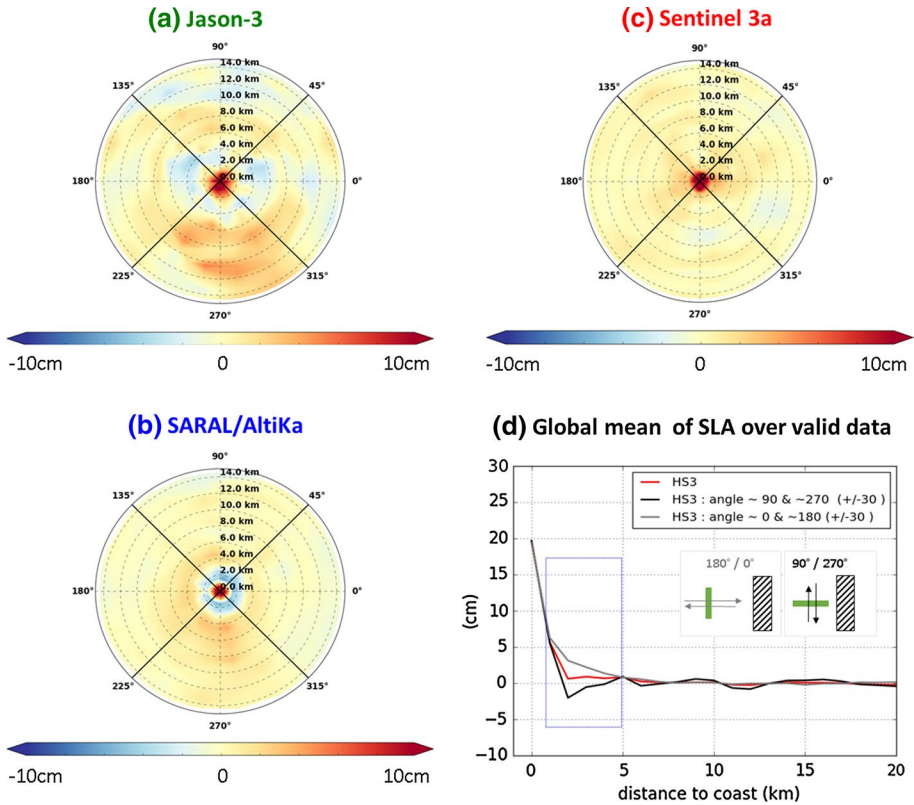


Fig. 6 Global average of the SLA derived from Jason-3, SARAL/AltiKa, and Sentinel-3A datasets (respectively, **a–c**). For the three first plots, the radius of the circle corresponds to the distance of the measurement from the closest coast line. The perimeter of the circle corresponds to the angle formed between the ground track of the satellite and the closest coastline. 0° and 180° angles correspond to a perpendicular approach, whereas 90° and 270° angles correspond to parallel displacement. Plot **d** is a one-dimensional representation of the Sentinel-3A SARM SLA average as a function of the distance to the coast in the global case (red curve) in the optimal case (gray curve) and in the worst case (black curve)

of optimal Sentinel-3A ground tracks (in perpendicular configuration with respect to the coastline) would allow us to compute relevant SSH measurements very close to the coast.

The diagnoses presented in this section mainly addressed the altimeter performances in the last 20 km band from the coast. Of course, the definition of coastal areas is not restricted to that narrow coastal strip; it also includes all the complex, regionally specific oceanic processes that could occur at hundreds of kilometers from the coast. We are confident in the altimeter capabilities to sample the large-scale and mesoscale signals in such areas. However, further work is needed to precisely describe their performances in order to exploit the shorter wavelengths.

6 A Selection of Coastal Altimetry Improvements

A number of studies in recent years have demonstrated the improvements in both quantity of valid measurements and quality as a function of distance from coast when waveforms are reprocessed and corrections optimized. Today, retracked pulse-limited altimetry, with optimized corrections, provides valid measurements to within 5 km from the coastline (Cipollini et al. 2017a, b).

The intrinsic capabilities of the innovative AltiKa Ka-band altimetry have confirmed expectations that, compared to conventional altimetry, the standard deviation of the range remains stable for AltiKa (lower than 10 cm) to less than 5 km from the coastline (Cipollini et al. 2017a, b). Much progress has been also achieved in assessing the quantity and quality of AltiKa sea level in coastal regions (Troupin et al. 2015).

The inherent improved capability of SAR mode in the coastal zone confirms that sea level is less noisy and more data are retained. The standard deviation of SLAs, which increases near coast, is the smallest for SAR data processed with SAMOSA+ (SAR Altimetry MOde Studies and Applications) and within the expected range until 2–3 km from the coast (Fenoglio-Marc et al. 2019). The accuracy of high-resolution along-track SLA from CryoSat-2 in SAR mode is in line with pulse-limited SARAL/AltiKa (Fenoglio-Marc et al. 2015; Gómez-Enri et al. 2018), and expected with Sentinel-3A and Sentinel-3B too.

Several studies have dealt with the comparison of various altimetric data sets with independent measurements (Xu et al. 2018; Vu et al. 2018) as well as the quality assessment of Sentinel-3A and CryoSat-2 (e.g., Bonnefond et al. 2018) and AltiKa data (Bonnefond et al. 2018). After 10 years of validation of coastal altimetry products in the Gulf of Cadiz and the Strait of Gibraltar (southwestern Iberian peninsula), the results clearly show that coastal-oriented retracking techniques (such as Adaptive Leading Edge Subwaveform (ALES)) and more accurate corrections provide around 20% of RMSE improvement for the high-resolution along-track SLA reprocessed using ALES retracker with respect to the operational GDR (Gómez-Enri et al. 2016). The comparison of sea level trends for tide gauges and the nearest along-track altimeter point shows some agreements but also some challenging discrepancies (Gharineiat and Deng 2018) when using along-track 1-Hz data supplied by the Radar Altimeter Database System (RADS) (Scharroo et al. 2013).

7 A Selection of Coastal Altimetry Applications

The availability of new experimental coastal altimetry products stimulated their usage for oceanographic studies (e.g., Birol et al. 2017). We will show a few examples to illustrate the contribution of coastal altimetry to sea level research studies in the coastal zone.

An improved coastal altimetry data set of sea level allowed the study of the flow variability through the Strait of Gibraltar (Gómez-Enri et al. 2019a). The study showed that global tidal models have in this region performances very close to a local model. However, in other regions global tidal models might not reproduce properly the tidal field. On the other hand, global MSS models in complex regions such as the Strait of Gibraltar show that residual errors may mask some of the sea level variability, making difficult its oceanographic interpretation. In the same area of investigation, Gómez-Enri et al. (2019b) show that sea level cross-strait differences are significantly correlated with zonal winds when a local along-track MSS based on ERS and Envisat retracked data is used instead of MSS models.

Regional studies of coastal sea level variability are other applications of coastal altimetry. For example, coastal altimetry datasets have revealed higher annual amplitudes in the presence of narrow coastal currents (Passaro et al. 2015, 2016), improved the knowledge of coastal tides (Piccioni et al. 2018) and permitted the extraction of coastal tidal mixing front signals (Dong et al. 2018).

Coastal altimetry plays also a critical role in storm surge forecasting studies. The value of improved altimeter data in capturing storm surges, if the satellite passes over the area at the right time, has been demonstrated by many authors. For example, Antony et al. (2014) analyzed altimeter data from the various missions in the Bay of Bengal during storm surge events. By coincidence, the Chinese HY2-A satellite passed at the right time to be above hurricane Sandy. The altimeter measured a storm surge of almost 1.5 m, with significant wave heights of nearly 8 m, making it the largest surge to date to be captured by satellite altimetry (Lillibridge et al. 2013). Coastal altimetry data have also been used for defining initial conditions in storm surge models to improve model performances in forecasting sea level peaks in the Venice region (Bajo et al. 2017) and in the Baltic Sea (Madsen et al. 2015).

Sea-level rise is seriously impacting coasts and coastal communities globally (Wright et al. 2018). For instance, in the Mediterranean Sea, the risk due to storm surges and coastal erosion under high sea level rise places vast portions of European coastline and United Nations Educational, Scientific and Cultural Organization (UNESCO) heritage sites at risk. It is thus important to have accurate sea-level observations in these sites in order to better assess the climate-related contribution. Tide gauge trends account for not only water volume changes but also land subsidence, which is observable using different techniques (e.g., GNSS, InSAR) in a limited number of sites. Coastal altimetry is aiming at extending the sea level climate record to the coastal zone with quality comparable to open ocean, thus contributing to answer the question if the sea level rate is similar or differs between open-ocean and the coastal zones. An example is the case of city of Venice, where the long-term implications of sea level rise have not been thoroughly investigated yet, and the contribution of the various processes to the coastal sea level change has not been noticeably quantified. A preliminary analysis of sea level changes around Venice (Vignudelli et al. 2019) shows that smaller trend has been found from altimetry (4.25 ± 1.25 mm/year) than those measured offshore (5.65 ± 1.25 mm/year) and in the lagoon (5.29 ± 1.27 mm/year), all local trends being much higher than that for the global mean sea level (GMSL) which is around 3.3 mm/year (Legeais et al. 2018). The differences might be explained in terms of VLM. However, the coastal zone needs specific processing, and the increased uncertainty in this area is not reflected in the trend error in the present version of the sea level CCI, which is based on open-ocean altimetry.

The new coastal altimetry datasets have many other uses as well. An example is the analysis of the surface signature due to a heavy Guadalquivir River discharge event (Gómez-Enri et al. 2018). The freshwater input will reduce the salinity levels in the surface layer during these episodes, resulting in a bump in the along-track CryoSat-2 sea level profile. Piecuch et al. (2018) highlighted the importance to get accurate satellite-based sea level measurements within a few kms of the coast and in estuaries (Durand et al. 2019). The analysis of river levels and tidal measurements from gauges installed throughout the eastern USA clearly illustrates that variations in river discharge can raise or lower coastal mean sea level by several centimeters.

Another study shows how the sparse coverage of tide gauges and their potential discontinuity in measuring sea level limit the accurate assessment of long-term changes in important coastal regions, such as the Pearl River delta (He et al. 2014) and that the

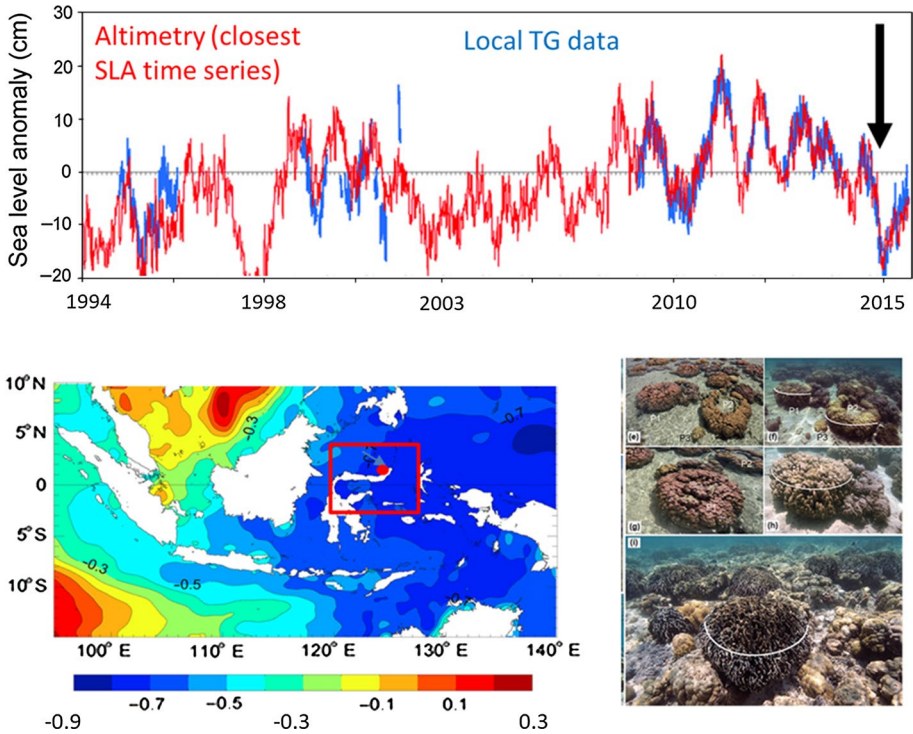


Fig. 7 Lower panel left: Bunaken location in the north of Sulawesi (Indonesia). Lower panel right: Bunaken reef flats and close-up of various coral colonies in **a–i**. Upper panel: SLAs measured by the Bitung tide gauge (TG) station (low-quality data), and overlaid on altimetry ADT anomaly data for the 1993–2016 period. To be noted the gaps in the tide gauge time series. Adapted from Ampou et al. (2017)

synergy with coastal altimetry data can contribute to reconstruct regionally consistent SLAs.

High-resolution coastal altimeter data are being used to monitor areas where recent mortality in coral communities was observed after an El Niño-induced sea level fall. For instance on Bunaken Island (Indonesia), radar altimetry and tide gauge data showed a rapid and significant sea level fall (Fig. 7), with a clear link to mortality (Ampou et al. 2017).

The new SARin mode operating on CryoSat-2 offers an additional possibility of discriminating land contamination signals from off-nadir land targets over coastal regions, thus helping to interpret sea level changes in complex morphologies. Idžanović et al. (2018) used SARin data to demonstrate the potential improvement of coastal sea level estimates around Norwegian coasts that are characterized by the presence of many islands, mountains, and deep, narrow fjords.

8 Perspectives from New Altimetry Missions

The space agencies are currently developing long-term scenarios aiming at filling gaps and satisfying emerging priority user needs. The coastal zone has two specific requirements in terms of spatial variability due to local effects and temporal evolution due to short events. The present constellation of eight altimeters provides an advantage for that type of monitoring. Coastal altimetry is a legitimate component of the coastal observing system (Benveniste et al. 2019) and now part of the new processing platforms, which allow researchers to rapidly process Earth observation data (Clerc et al. 2016). From a technological point of view, there will be a consolidation of the SAR mode in future radar altimeters and an important change of paradigm using SAR interferometry with radar altimetry becoming an imaging sensor.

8.1 SAR Altimetry

The recent developments in SAR mode toward higher resolution (up to 300 m along track) that contributed to the scientific advancement for coastal sea level studies will continue with forthcoming Sentinel-3C/D and Sentinel-6A/B. Those missions will be based on the heritage of previous Sentinel-3A and Sentinel-3B. An important innovation in Sentinel-6 will be the adoption of the continuous high-rate pulse mode (interleaved mode), compared to the closed burst mode used on Sentinel-3 and CryoSat-2 missions. Additionally, Sentinel-6A and Sentinel-6B will perform simultaneously LRM and SAR mode measurements, which will permit a very-high-accuracy link to the previous reference missions (TOPEX/Poseidon and Jason series). It is also important to mention the SKIM (Sea surface Kinematics Multiscale monitoring), which is an ESA-EE9 candidate satellite mission that would carry on board a radar altimeter and adopt a processing of the nadir beam similar to Sentinel-3C/D and Sentinel-6A/B (Ardhuin et al. 2019).

The Envisat radar altimeter made available individual echoes (IE) in bursts of a maximum of 2000 complex echo samples (1.114 s) every 3 min. SARAL includes a similar capability. These individual echoes with higher spatial resolution (every 3.8 m along the ground track) opened new ways in processing and extracting the very detailed information encoded in them (Abileah et al. 2013), stimulating the development of further research (Abileah et al. 2017), and now applicable to CryoSat-2 (SAR and SARin modes) and Sentinel-3 where individual echoes come in short burst with 89 m ground spacing (Abileah et al. 2017).

A recommendation made by the radar altimetry community during the Ocean Surface Topography Science Team Meeting in Venice, Italy, in 2012, was to consider a second radiometer for future operational altimetry missions such as next-generation Sentinel missions to operate at high frequencies to resolve km-scale water vapor to improve coastal altimetry applications. A multi-frequency radiometer antenna and feed system that could provide such accurate atmospheric corrections will be included on the Sentinel-6 mission.

The so-called Copernicus Space Component (CSC) Expansion program has identified a Polar Ice and Snow Topographic Mission. This mission will provide enhanced retrieval of land ice sheet/glacier elevation, sea ice thickness and freeboard as well as ocean surface elevation, wave height and wind speed by higher spatial resolution measurements. The primary high-level objectives are to monitor critical climate signals: ice sheet, ice cap melting and sea level, as well as to monitor variability of Arctic and Southern Ocean sea ice and

its snow-loading. Other objectives are to support applications related to coastal and inland waters and contribute to the observation of ocean topography.

A study concerning the Copernicus long-term scenario (jointly developed by ESA-EC-EUMETSAT) has just started to prepare the Copernicus next generation of satellite missions. The vision is to have the topographic measurement family supporting operational oceanography ensuring enhanced continuity of Sun-synchronous (Sentinel-3) and enhanced continuity of reference mission (Sentinel-6) as well as complementary polar orbiting mission for enhanced ice monitoring.

8.2 Interferometry on the Surface Water and Ocean Topography (SWOT) mission

8.2.1 Introduction

The present altimetric constellation includes conventional missions and missions with new SAR (along-track) and SAR-Interferometry (along-track and cross-track) technology that provide enhanced spatial resolution of the observations of SSH. Such capability has improved the spatial resolution near the coast over conventional altimetry. The benefit of SAR mode is already demonstrated, especially when the satellite approaches the coast at a perpendicular angle, maximizing the resolution by the SAR sampling and processing, while in the across-track direction the expected improvements are not observed, although at present the analyses are at early stage (as already explained in Sect. 3). The advantage of SAR-Interferometry along-track only recently started with some studies [e.g., Abulaitijiang et al. (2015) show that data from 0 to 7 km inland can be re-allocated to the coast using the off-nadir range correction]. Despite the current constellation in orbit, the major limitation of altimeter satellites is related to its nadir only sampling. There is clearly a need to

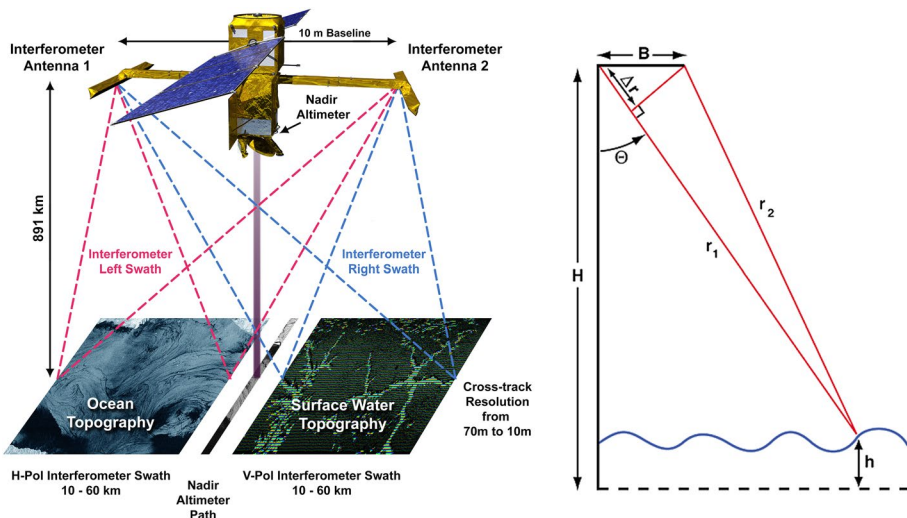


Fig. 8 The measurement system of SWOT is shown on the left. The two interferometer antennae, part of the Ka-Band Radar Interferometer (KaRIN), are separated by a 10-m mast. Each will transmit and receive radar signals. The signals received by the two antennae from the same target will allow the performance of interferometry as shown on the right. See text for explanations

improve the spatial and temporal sampling of those complex zones by providing 2D maps of the SSH.

In the future, two-dimensional wide-swath observations of the ocean surface topography will be made from the international Surface Water and Ocean Topography (SWOT) Mission (Fu and Ubelmann 2014), planned for launch in 2021. SWOT will make high-resolution observations using the SAR radar interferometry technique (Fig. 8). Two SAR antennae will be carried on board at the ends of a rigid mast 10 m long. The phase difference between the signals received by the two antennae allows the determination of the height of sea surface,

$$h = H - r_1 \cos(\theta) \quad (1)$$

The error of h can be expressed

$$\delta h = r_1 \lambda \tan(\theta) \frac{\delta \varphi}{2\pi B} \quad (2)$$

To minimize the height error, both the radar wavelength, λ , and look angle, ϑ , should be small. For SWOT, the wavelength as chosen to be Ka-band, ~ 1 cm, the look angle is near nadir, 0.4° – 4° (compromise between ocean and inland water needs), forming a swath from 10 to 60 km from the nadir on each side of the nadir track for an altitude of 891 km of the spacecraft.

With measurements over a swath of 120 km (20 km nadir gap), SWOT will map the entire Earth within $\pm 77.6^\circ$ latitudes with a repeat cycle of 21 days after a 3-month Cal/Val phase with a repeat cycle of 1 day. Over the ocean, these new measurements will extend the two-dimensional resolution of ocean surface topography estimated from conventional radar altimetry from 150 km wavelength to possibly 15 km (Fu and Ubelmann 2014), offering opportunities to observe the oceanic dynamic processes at these scales that act as one of the main gateways connecting the interior of the ocean to the upper layer. These processes provide both sinks and sources for the kinetic energy at larger scales, involving both low-frequency geostrophically balanced motions and high-frequency internal tides and gravity waves (Qiu et al. 2018). The active vertical exchanges linked to these scales are a key aspect of the role of the ocean in the climate system. These vertical exchanges have impacts on the local and global budgets of heat, carbon and nutrients for biogeochemical cycles (Klein and Lapeyre 2009).

8.2.2 Measurement Requirements

Figure 9 is the measurement performance requirement in the form of the wavenumber spectra of SSH signals and measurement errors (Rodríguez 2016). The spatial resolution is defined as the wavelength where the signal intersects with the error. Approximately over 68% of the ocean, the resolution is expected to be about 15 km under 2 m SWH. The measurement noise increases with SWH, making the SWOT resolution seasonally and geographically dependent (Wang et al. 2019).

Figure 10 is a plot of the height error over water bodies on land as function of the area over which the data are averaged to the area indicated (Desai 2018). It should be valid for estuaries and coastal waters not contaminated by land. The error increases with decreasing amount of averaging, reaching 0.5 m for an area of 100 m \times 100 m. In coastal zones, the

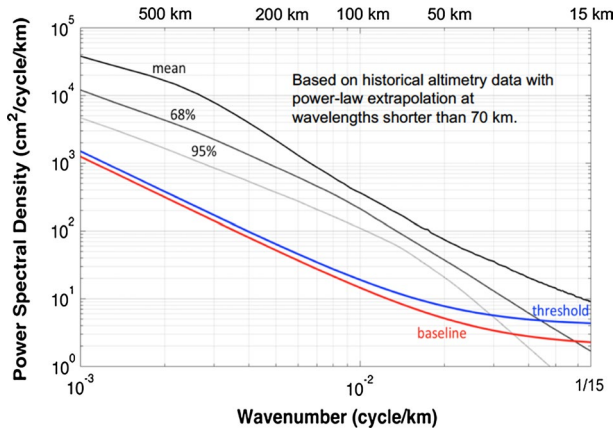


Fig. 9 SSH baseline requirement spectrum (red curve) as a function of wavenumber. Blue curve is the threshold requirement. Shown, for reference, is the global mean SSH spectrum estimated from the Jason-1 and Jason-2 observations (thick black line), the lower boundary of 68% of the spectral values (the upper gray dotted line), and the lower boundary of 95% of the spectral values (the lower gray dotted line). The intersections of the two dotted lines with the baseline spectrum at ~ 15 km (68%) and ~ 30 km (95%) determine the resolving capabilities of the SWOT measurement. The respective resolution for the threshold requirement is ~ 25 km (68%) and ~ 35 km (95%)

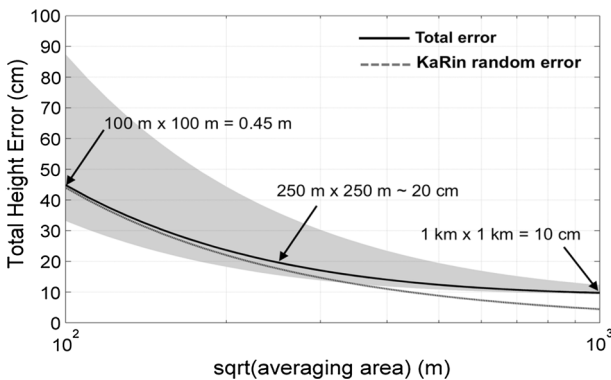


Fig. 10 Estimated non-vegetated water body total height accuracy for water-only pixels as a function of averaging area used to form the estimate (solid curve). Shown, for reference, is the KaRIN random error only contribution to the height accuracy (dashed curve). The total height accuracy is 10 cm for an equivalent water area of 1 km², 21 cm for (250 m)², and 50 cm for (100 m)². Due to changes in spatial resolution and signal-to-noise ratio, the performance will vary across the swath. The shaded area shows the expected variability in performance as a function of the averaging area

small size of the resolved pixels, on the order of 50 m, allows water detection without land contamination as in the case of conventional altimeters. The two-dimensional mapping of water bodies will enable the tackling of many coastal processes, such as inundation from storm surges, the interaction or river flow with the open ocean, etc.

8.2.3 A Fast-Sampling Phase for Calibration and Validation

To mitigate the challenge of the temporal sampling, the first 90 days of the mission after the commissioning phase for engineering checkout and adjustment will be flown in a 1-day repeat fast-sampling phase for calibration and validation.

This much-improved temporal sampling will allow enhanced understanding of the measurement at 15–150 km wavelengths in terms of signals and measurement errors. In particular, there will be two measurements a day at the crossover diamond-shaped regions, where the two-dimensional measurement at twice daily interval will provide the maximum amount of information on rapidly changing signals and errors. During the calibration and validation phases, in situ observations of the dynamic height of the ocean will be deployed to evaluate the relationship of the SSH measurement to the internal processes of the ocean. An airborne LiDAR system will also be flown to measure the SSH for comparison to the satellite observations.

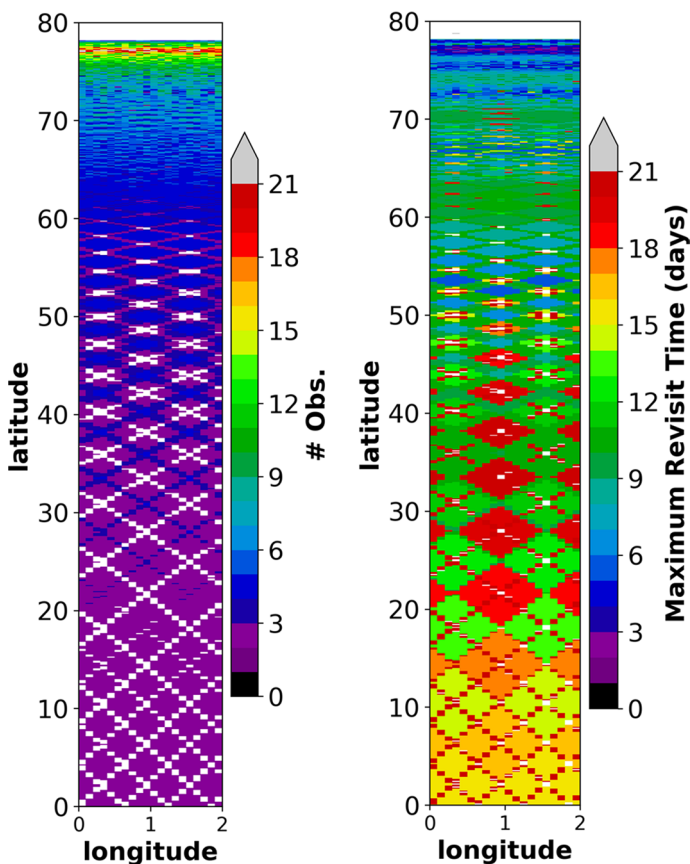


Fig. 11 Sampling pattern of the 21-day orbit for the Science Phase. The left panel shows the number of observations at a given location during the 21-day repeat period. The right panel shows the maximum gap in days between two successive observations

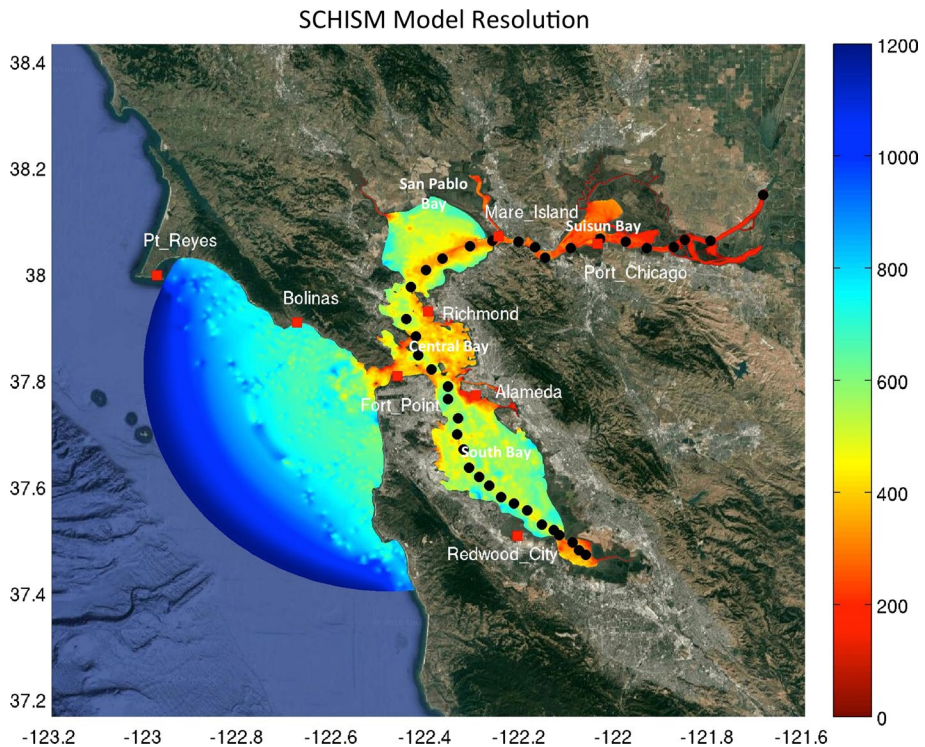


Fig. 12 The color shades of the map show the SCHISM model domain and spatial resolution (meters) of the San Francisco Bay configuration. The black dots show the locations of 37 USGS water quality monitoring stations; the red squares show the locations of tide gauge stations. Adapted from Chao et al. (2017)

8.2.4 Scientific Applications

The SWOT mission's topics of oceanographic investigations cover mesoscale and sub-mesoscale processes; modeling and data assimilation; tides, waves, and high-frequency processes; calibration and validation; coastal and estuarine processes. Because of the challenges posed by the coarse temporal sampling (Fig. 11) and measurement errors, it is expected that the science investigation will heavily depend on modeling and assimilation for the construction of high-level gridded products. Efforts are being made to meet the challenges, by modeling the low-frequency balanced motions and high-frequency tides and internal gravity waves and by testing the assimilation of SWOT-like data into the models with the aim of constructing the ocean state in both space and time.

In the coastal zones, SWOT will largely improve data resolution, coverage and accuracy to address problems of the interaction of estuaries and coastal oceans. Shown in Fig. 12 is illustration of such applications in the context of a high-resolution ocean model called Semi-implicit Cross-scale Hydroscience Integrated System Model (SCHISM) (Chao et al. 2017). The color shades of the map show the SCHISM model domain and spatial resolution (meters) of the San Francisco Bay configuration. The black dots show the locations of 37 United States Geological Survey (USGS) water quality monitoring stations; the red squares show the locations of tide gauge stations. SWOT data will have resolutions

progressing from scale of 1 km in the open ocean to ~ 100 m in the San Francisco Bay and upstream to the Sacramento River. The combination of data and modeling will allow studies of processes such as tidal mixing, storm surges and salt water intrusions.

9 Remaining Challenges and Concluding Remarks

A great progress has been made in coastal altimetry during the last decade to maintain as much as possible the open-ocean sea level accuracy while approaching the coast (Benveniste et al. 2019). Several approaches have been proposed to detect and take care of anomalous samples in waveforms collected from various pulse-limited altimetry missions, in particular in the strip of 10 km from the coast, bringing improvement in coastal sea level data. Recent technology advances in processing (SAR mode adopted in both CryoSat-2 and Sentinel-3 missions) already demonstrate that it is possible to enhance the quality and quantity of the sea level record close to the coast. Similarly, the better signal-to-noise ratio, smaller footprint, and high along-track sampling of SARAL/AltiKa acquire less-corrupted data, thus enhancing data availability in the 0–10 km coastal strip.

Beyond 10 km from the coast, users can benefit from recent coastal altimetry processing improvements (e.g., optimized geophysical corrections and high-resolution products). However, it is still a challenge to obtain accurate coastal sea levels in the 0–10 km band. Conventional altimetry still suffers from artifacts in the presence of complex coastal morphologies (e.g., steep relief, islands around, estuaries). SAR altimetry performances can be reliant on the angle the satellite approaches the coastline, with waveforms resulting contaminated and requiring dedicated retracking (Dinardo et al. 2018). Most of auxiliary information (orbit, ionosphere and tropospheric corrections, SSB) is still provided at standard rate (1 Hz). The need to have an SSB correction at 20 Hz and a specific SSB for each retracker has been highlighted (Pires et al. 2018). With retracked ranges and improved corrections, an enhanced MSS accuracy would be achieved because more and more accurate data would be available for the temporal averaging process. An inaccurate MSS might also mask some of the sea level variability making difficult the interpretation of oceanographic signals. The computation of some auxiliary information necessary to transform range in usable quantities (e.g., tidal and atmospheric corrections) requires models that, however, still use coarse bathymetry. There is a need to enhance bathymetry in order to increase the accuracy of those models in the coastal zone.

The continuous improvement in data processing and the recent progress in technology have allowed the development of various experimental coastal altimetry products suitable for coastal zone studies, which are now validated and being used for sea level research. The contribution of coastal altimetry is considered essential to within 0–10 km to link the sea level changes derived from the altimetry with those observed at tide gauges (Ponte et al. 2019). As the sampling of a single altimeter cannot be optimized to observe the complex variability of sea level at coastal scale, the merging of different missions that accounts for usage of 20 Hz high-resolution data, requires rethinking the typical grid approach used with 1 Hz data to downscale data at higher resolution from open ocean to coasts. Wide-swath altimetry that will be embarked for the first time on SWOT mission and envisaged for Sentinel-3 new generation will largely improve the temporal and spatial sampling of those complex zones.

Acknowledgements Thanks go to the European Space Agency that supported the development and exploitation of coastal altimetry with various scientific projects (COASTALT, Contract No. 21201/08/I-LG;

eSurge Venice, Contract No. 4000104485/11/I-LG; C-TEP, Contract No. C_TEP.1313.ACR-CNR.i1r0; CCI+ Bridging phase, Contract No. 4000109872/13/I-NB; SCOOP, Contract No. 4000115385/15/I-BG and that has organized and financially supported the gathering of the Coastal Altimetry Community with regular Coastal Altimetry Workshops in the past 10 years.

References

- Abileah R, Gómez-Enri J, Scozzari A, Vignudelli S (2013) Coherent ranging with Envisat radar altimeter: a new perspective in analyzing altimeter data using Doppler processing. *Remote Sens Environ* 139:271–276. <https://doi.org/10.1016/j.rse.2013.08.005>
- Abileah R, Scozzari A, Vignudelli S (2017) Envisat RA-2 individual echoes: a unique dataset for a better understanding of inland water altimetry potentialities. *Remote Sens* 9(6):605. <https://doi.org/10.3390/rs9060605>
- Ablain M, Legeais JF, Prandi P, Marcos M, Fenoglio-Marc L, Dieng HB, Benveniste A, Cazenave A (2017) Satellite altimetry-based sea level at global and regional scales. In: Cazenave A, Champollion N, Paul F, Benveniste J (eds) *Integrative study of the mean sea level and its components*, vol 58. Space sciences series of ISSI. Springer, Cham, pp 9–33. https://doi.org/10.1007/978-3-319-56490-6_2
- Abulaitijiang A, Andersen OB, Stenseng L (2015) Coastal sea level from inland CryoSat-2 interferometric SAR altimetry. *Geophys Res Lett* 42(6):1841–1847. <https://doi.org/10.1002/2015GL063131>
- Ampou EE, Johan O, Menkes CE, Niño F, Birol F, Ouillon S, Andréfouët S (2017) Coral mortality induced by the 2015–2016 El-Niño in Indonesia: the effect of rapid sea level fall. *Biogeosciences* 14(4):817–826. <https://doi.org/10.5194/bg-14-817-2017>
- Andersen OB, Scharroo R (2011) Range and geophysical corrections in coastal regions: and implications for mean sea surface determination. In: Vignudelli S, Kostianoy A, Cipollini P, Benveniste J (eds) *Coastal altimetry*. Springer, Berlin, pp 103–146. https://doi.org/10.1007/978-3-642-12796-0_5
- Antony C, Testut L, Unnikrishnan AS (2014) Observing storm surges in the Bay of Bengal from satellite altimetry. *Estuar Coast Shelf Sci* 151:131–140. <https://doi.org/10.1016/j.ecss.2014.09.012>
- Arduin F, Brandt P, Gaultier L, Donlon C, Battaglia A, Boy F, Casal T, Chapron B, Collard F, Cravatte S, Delouis JM (2019) SKIM, a candidate satellite mission exploring global ocean currents and waves. *Front Mar Sci* 6(209):1–8. <https://doi.org/10.3389/fmars.2019.00209>
- Bajo M, De Biasio F, Umgiesser G, Vignudelli S, Zecchetto S (2017) Impact of using scatterometer and altimeter data on storm surge forecasting. *Ocean Model* 113:85–94. <https://doi.org/10.1016/j.ocemo.2017.03.014>
- Benveniste J, Cazenave A, Vignudelli S, Fenoglio-Marc L, Shah R, Almar R, Andersen O, Birol F, Bonnefond P, Bouffard J, Calafat F, Cardellach E, Cipollini P, Dufau C, Fernandes J, Garrison J, Frappart F, Gommenginger C, Han G, Høyér JL, Kourafalou V, Le Cozannet G, Leuliette E, Li Z, Loisel H, Madsen KS, Marcos M, Melet A, Meyssignac B, Passaro M, Pasqual A, Passaro M, Ribo S, Scharroo R, Song T, Speich S, Wilkin J, Woodworth P, Wöppelmann G (2019) Requirements for a coastal hazard observing system. *OceanObs'19 community white paper*. *Front Mar Sci J Spec Sect Coast Ocean Process* 6:348. <https://doi.org/10.3389/fmars.2019.00348>
- Berry PAM, Freeman JA, Smith RG (2010) An enhanced ocean and coastal zone retracking technique for gravity field computation. In: Mertikas SP (ed) *Gravity, geoid and Earth observation International Association of Geodesy Symposia*, vol 135. Springer, Berlin, pp 213–220. https://doi.org/10.1007/978-3-642-10634-7_28
- Birgiel E, Ellmann A, Delpeche-Ellmann N (2018) Examining the performance of the Sentinel-3 coastal altimetry in the Baltic Sea using a regional high-resolution geoid model. In: *Proceedings of 2018 Baltic geodetic congress (BGC Geomatics)*, Olsztyn, Poland, 21–23 June 2018. <https://doi.org/10.1109/bgc-geomatics.2018.00043>
- Birol F, Roblou L, Lyard F, Llovel W, Durand F, Renault L, Dewitte R, Morrow R, Ménard Y (2006) Towards using satellite altimetry for the observation of coastal dynamics. In: Danesy D (ed) *Proceedings of 15 years of progress in radar altimetry joint ESA-CNES symposium*, Venice, Italy, 13–18 March 2006, ESA SP-614. ISBN: 92-9092-925-1
- Birol F, Fuller N, Lyard F, Cancet M, Nino F, Delebecque C, Fleury S, Toubanc F, Melet A, Saraceno M, Léger F (2017) Coastal applications from nadir altimetry: example of the X-TRACK regional products. *Adv Space Res* 59(4):936–953. <https://doi.org/10.1016/j.asr.2016.11.005>
- Bonnefond P, Verron J, Aublanc J, Babu KN, Bergé-Nguyen M, Cancet M, Chaudhary A, Crétaux JF, Frappart F, Haines BJ, Laurain O, Ollivier A, Poisson JC, Prandi P, Sharma R, Thibaut P, Watson

- C (2018) The benefits of the Ka-band as evidenced from the SARAL/Altika altimetric mission: quality assessment and unique characteristics of Altika data. *Remote Sens* 10(1):83. <https://doi.org/10.3390/rs10010083>
- Boy F, Desjonquères J-D, Picot N, Moreau T, Raynal M (2017) CryoSat-2 SAR-mode over oceans: processing methods, global assessment, and benefits. *IEEE Trans Geosci Remote Sens* 55(1):148–158. <https://doi.org/10.1109/TGRS.2016.2601958>
- Brown G (1977) The average impulse response of a rough surface and its applications. *IEEE Trans Antennas Propag* 25(1):67–74. <https://doi.org/10.1109/TAP.1977.1141536>
- Brown S (2010) A novel near-land radiometer wet path-delay retrieval algorithm: application to the Jason-2/OSTM advanced microwave radiometer. *IEEE Trans Geosci Remote Sens* 48(4):1986–1992. <https://doi.org/10.1109/TGRS.2009.2037220>
- Carrère L, Lyard F (2003) Modeling the barotropic response of the global ocean to atmospheric wind and pressure forcing-comparisons with observations. *Geophys Res Lett*. <https://doi.org/10.1029/2002g1016473>
- Carrere L, Faugère Y, Ablain M (2016) Major improvement of altimetry sea level estimations using pressure-derived corrections based on ERA-Interim atmospheric reanalysis. *Ocean Sci* 12:825–842. <https://doi.org/10.5194/os-12-825-2016>
- Cazenave A, Palanisamy H, Ablain M (2018) Contemporary sea level changes from satellite altimetry: what have we learned? What are the new challenges? *Adv Space Res* 62(7):1639–1653. <https://doi.org/10.1016/j.asr.2018.07.017>
- Chao Y, Farrara JD, Zhang H, Zhang YJ, Atelijevec E, Chai F, Davis CO, Dugdale R, Wilkerson F (2017) Development, implementation, and validation of a modeling system for the San Francisco Bay and Estuary. *Estuar Coast Shelf Sci* 194:40–56. <https://doi.org/10.1016/j.ecss.2017.06.005>
- Cipollini P, Vignudelli S, Benveniste J (2014) The coastal zone: a mission target for satellite altimeters. *EOS Trans AGU* 95(8):72. <https://doi.org/10.1002/2014EO080006>
- Cipollini P, Calafat FM, Jevrejeva S, Melet A, Prandi P (2017a) Monitoring sea level in the coastal zone with satellite altimetry and tide gauges. *Surv Geophys* 38:33–57. <https://doi.org/10.1007/s10712-016-9392-0>
- Cipollini P, Benveniste J, Birol F, Fernandes MJ, Obligis E, Passaro M, Strub PT, Valladeau G, Vignudelli S, Wilkin J (2017b) Satellite altimetry in coastal regions. In: Stammer D, Cazenave A (eds) *Satellite altimetry over oceans and land surfaces*. CRC Press, Boca Raton, FL, pp 343–380
- Clerc S, O' Mahony C, Mangin A, Dacu M, Vignudelli S, Illuzzi D, Craciunescu V, Leone R, Campbell G (2016) New perspectives for the observation of coastal zones with the Coastal Thematic Exploitation Platform. In: *Proceedings of European Space Agency living planet symposium*, 9–13 May 2016, Prague, Czech Republic, ESA SP 740, August 2016
- Cotton PD, Garcia PN, Cancet M, Andersen O, Stenseng L, Martin F, Cipollini P, Calafat FM, Passaro M, Ambrózio A, Benveniste J (2016) Improved oceanographic measurements with cryosat sar altimetry: application to the coastal zone and arctic. In: *Proceedings of European Space Agency living planet symposium*, 9–13 May 2016, Prague, Czech Republic, ESA SP 740, August 2016
- Deng X, Featherstone WE (2006) A coastal retracking system for satellite radar altimeter waveforms: application to ERS-2 around Australia. *J Geophys Res Oceans*. <https://doi.org/10.1029/2005jc003039>
- Desai S (2018) Surface water and ocean topography mission (SWOT) project. Science requirements doc., revision B. California Institute of Technology Jet Propulsion Laboratory Publ. JPL D-61923
- Desjonquères J, Carayon G, Steunou N, Lambin J (2010) Poseidon-3 radar altimeter: new modes and in-flight performances. *Mar Geod* 33(Suppl.):57–79. <https://doi.org/10.1080/01490419.2010.488970>
- Desportes C, Obligis E, Eymard L (2007) On the wet tropospheric correction for altimetry in coastal regions. *IEEE Trans Geosci Remote Sens* 45(7):2139–2149. <https://doi.org/10.1109/TGRS.2006.888967>
- Dinaro S, Fenoglio-Marc L, Buchhaupt C, Becker M, Scharroo R, Fernandes MJ, Benveniste J (2018) Coastal SAR and PLRM altimetry in German Bight and West Baltic Sea. *Adv Space Res* 62(6):1371–1404. <https://doi.org/10.1016/j.asr.2017.12.018>
- Dong C, Xu G, Han G, Chen N, He Y, Chen D (2018) Identification of tidal mixing fronts from high-resolution along-track altimetry data. *Remote Sens Environ* 209:489–496. <https://doi.org/10.1016/j.rse.2018.02.047>
- Durand F, Piecuch CG, Becker M, Papa F, Raju SV, Khan JU, Ponte RM (2019) Impact of continental freshwater runoff on coastal sea level. *Surv Geophys*. <https://doi.org/10.1007/s10712-019-09536-w>
- Egido A, Smith WH (2017) Fully focused SAR altimetry: theory and applications. *IEEE Trans Geosci Remote Sens* 55(1):392–406. <https://doi.org/10.1109/TGRS.2016.2607122>

- Emery KO, Aubrey DG (eds) (1991) Sea levels, land levels, and tide gauges. Springer, Berlin. <https://doi.org/10.1007/978-1-4613-9101-2>
- Fenoglio-Marc L, Dinardo S, Scharroo R, Roland A, Sikiric MD, Lucas B, Becker M, Benveniste J, Weiss R (2015) The German bight: a validation of CryoSat-2 altimeter data in SAR mode. *Adv Space Res* 55(11):2641–2656. <https://doi.org/10.1016/j.asr.2015.02.014>
- Fenoglio-Marc L, Dinardo S, Buchhaupt C, Scharroo R, Becker M, Benveniste J (2019) Calibrating the SAR sea surface heights of CryoSat-2 and Sentinel-3 along the German coasts. In: *Proceedings of international association of geodesy symposia*. Springer, Berlin. https://doi.org/10.1007/1345_2019_73
- Fernandes MJ, Lázaro C (2016) GPD+ wet tropospheric corrections for CryoSat-2 and GFO altimetry missions. *Remote Sens* 8(10):851. <https://doi.org/10.3390/rs8100851>
- Fernandes MJ, Pires N, Lázaro C, Nunes AL (2013) Tropospheric delays from GNSS for application in coastal altimetry. *Adv Space Res* 51(8):1352–1368. <https://doi.org/10.1016/j.asr.2012.04.025>
- Fernandes MJ, Lázaro C, Nunes AL, Scharroo R (2014) Atmospheric corrections for altimetry studies over inland water. *Remote Sens* 6(6):4952–4997. <https://doi.org/10.3390/rs6064952>
- Fernandes MJ, Lázaro C, Ablain M, Pires N (2015) Improved wet path delays for all ESA and reference altimetric missions. *Remote Sens Environ* 169:50–74. <https://doi.org/10.1016/j.rse.2015.07.023>
- Fu LL, Cazenave A (eds) (2001) *Satellite altimetry and earth sciences: a handbook of techniques and applications*. Academic Press, London
- Fu L-L, Ubelmann C (2014) On the transition from profile altimeter to swath altimeter for observing global ocean surface topography. *J Ocean Atmos Technol* 31(2):560–568. <https://doi.org/10.1175/JTECH-D-13-00109.1>
- García P, Martín-Puig C, Roca M (2018) SARin mode, and a window delay approach, for coastal altimetry. *Adv Space Res* 62(6):1358–1370. <https://doi.org/10.1016/j.asr.2018.03.015>
- Gharineiat Z, Deng X (2018) Description and assessment of regional sea-level trends and variability from altimetry and tide gauges at the northern Australian coast. *Adv Space Res* 61(10):2540–2554. <https://doi.org/10.1016/j.asr.2018.02.038>
- Gómez-Enri J, Vignudelli S, Quartly G, Gommenginger C, Benveniste J (2009) Bringing satellite radar altimetry closer to shore. In: *SPIE (Society of Photo-Optical Instrumentation Engineers) News-room*, pp 1–3. <https://doi.org/10.1117/2.1200908.1797>
- Gómez-Enri J, Vignudelli S, Quartly GD, Gommenginger CP, Cipollini P, Challenor PG, Benveniste J (2010) Modeling ENVISAT RA-2 waveforms in the coastal zone: case study of calm water contamination. *IEEE Geosci Remote Sens Lett* 7(3):474–478. <https://doi.org/10.1109/LGRS.2009.2039193>
- Gómez-Enri J, Cipollini P, Passaro M, Vignudelli S, Tejedor B, Coca J (2016) Coastal altimetry products in the strait of Gibraltar. *IEEE Trans Geosci Remote Sens* 54(9):5455–5466. <https://doi.org/10.1109/tgrs.2016.2565472>
- Gómez-Enri J, Vignudelli S, Cipollini P, Coca J, González CJ (2018) Validation of CryoSat-2 SIRAL sea level data in the eastern continental shelf of the Gulf of Cadiz (Spain). *Adv Space Res* 62(6):1405–1420. <https://doi.org/10.1016/j.asr.2017.10.042>
- Gómez-Enri J, González CJ, Passaro M, Vignudelli S, Álvarez O, Cipollini P, Mañanes R, Bruno M, Lopez-Carmona P, Izquierdo A (2019a) Wind-induced cross-strait sea level variability in the Strait of Gibraltar using coastal altimetry and in-situ measurements. *Remote Sens Environ* 221:596–608. <https://doi.org/10.1016/j.rse.2018.11.042>
- Gómez-Enri J, Vignudelli S, Izquierdo A, Passaro M, González C J, Cipollini P, Bruno M, Álvarez O, Mañanes R (2019b) Sea level variability in the Strait of Gibraltar from along-track high spatial resolution altimeter products. In: *Proceedings of international association of geodesy symposia—international review workshop on satellite altimetry Cal/Val activities and applications*, 23–26 April 2018, Crete, Greece. Springer, Berlin, pp 1–10. https://doi.org/10.1007/1345_2019_54
- Guo J, Gao Y, Hwang C, Sun J (2010) A multi-subwaveform parametric retracker of the radar satellite altimetric waveform and recovery of gravity anomalies over coastal oceans. *Sci China Earth Sci* 53(4):610–616. <https://doi.org/10.1007/s11430-009-0171-3>
- Halpern BS, Frazier M, Potapenko J, Casey KS, Koenig K, Longo C et al (2015) Spatial and temporal changes in cumulative human impacts on the world’s ocean. *Nat Commun* 6:7615. <https://doi.org/10.1038/ncomms8615>
- Hauser D, Tison C, Amiot T, Delaye L, Corcoral N, Castillan P (2017) SWIM: the first spaceborne wave scatterometer. *IEEE Trans Geosci Remote Sens* 55(5):3000–3014. <https://doi.org/10.1109/TGRS.2017.2658672>
- He L, Li G, Li K, Shu Y (2014) Estimation of regional sea level change in the Pearl River Delta from tide gauge and satellite altimetry data. *Estuar Coast Shelf Sci* 141:69–77. <https://doi.org/10.1016/j.ecss.2014.02.005>

- Heslop EE, Sánchez-Román A, Pascual A, Rodríguez D, Reeve KA, Faugère Y, Raynal M (2017) Sentinel-3A views ocean variability more accurately at finer resolution. *Geophys Res Lett.* <https://doi.org/10.1002/2017GL076244>
- Hwang C, Hsu HY, Jang RJ (2002) Global mean sea surface and marine gravity anomaly from multi-satellite altimetry: applications of deflection-geoid and inverse Vening Meinesz formulae. *J Geod* 76(8):407–418. <https://doi.org/10.1007/s00190-002-0265-6>
- Idris NH, Deng X (2012) The retracking technique on multi-peak and quasi-specular waveforms for Jason-1 and Jason-2 missions near the coast. *Mar Geod* 35(sup1):217–237. <https://doi.org/10.1080/01490419.2012.718679>
- Idžanović M, Ophaug V, Andersen OB (2018) Coastal sea level from CryoSat-2 SARIn altimetry in Norway. *Adv Space Res* 62(6):1344–1357. <https://doi.org/10.1016/j.asr.2017.07.043>
- Klein P, Lapeyre G (2009) The oceanic vertical pump induced by mesoscale and submesoscale turbulence. *Annu Rev Mar Sci* 1:351–375. <https://doi.org/10.1146/annurev.marine.010908.163704>
- Kummu M, De Moel H, Salvucci G, Viviroli D, Ward PJ, Varis O (2016) Over the hills and further away from coast: global geospatial patterns of human and environment over the 20th–21st centuries. *Environ Res Lett* 11(3):034010. <https://doi.org/10.1088/1748-9326/11/3/034010>
- Labroue S, Gaspar P, Dorandeu J, Ogor F, Zanife OZ (2006) Overview of the improvements made on the empirical determination of the sea state bias correction. In: *Proceedings of 15 years of progress in radar altimetry symposium, Venice, 13–18 March, 2006, ESA SP614*
- Le Bars Y, Lyard F, Jeandel C, Dardengo L (2010) The AMANDES tidal model for the Amazon estuary and shelf. *Ocean Model* 31(3):132–149. <https://doi.org/10.1016/j.ocemod.2009.11.001>
- Legeais JF, Ablain M, Zawadzki L, Zuo H, Johannessen JA, Scharffenberg MG, Fenoglio-Marc L, Fernandes J, Andersen OB, Rudenko S, Cipollini P, Quartly GD, Passaro M, Cazenave A, Cipollini P (2018) An improved and homogeneous altimeter sea level record from the ESA climate change initiative. *Earth Syst Sci Data* 10:281–301. <https://doi.org/10.5194/essd-10-281-2018>
- LillibrIDGE J, Lin M, Shum CK (2013) Hurricane Sandy storm surge measured by satellite altimetry. *Oceanography* 26(2):8–9. <https://doi.org/10.5670/oceanog.2013.18>
- Madsen KS, Hoyer JL, Fu W, Donlon C (2015) Blending of satellite and tide gauge sea level observations and its assimilation in a storm surge model of the North Sea and Baltic Sea. *J Geophys Res Oceans* 120(9):6405–6418. <https://doi.org/10.1002/2015JC011070>
- Maraldi C, Galton-Fenzi B, Lyard F, Testut L, Coleman R (2007) Barotropic tides of the southern Indian Ocean and the Amery Ice Shelf cavity. *Geophys Res Lett.* <https://doi.org/10.1029/2007g1030900>
- Marcos M, Wöppelmann G, Matthews A, Ponte RM, Birol F, Arduin F, Coco G, Santamaría-Gómez A, Ballu V, Testut L, Chambers D, Stopa JE (2019) Coastal sea level and related fields from existing observing systems. *Surv Geophys.* <https://doi.org/10.1007/s10712-019-09513-3>
- Neumann B, Vafeidis AT, Zimmermann J, Nicholls RJ (2015) Future coastal population growth and exposure to sea-level rise and coastal flooding: a global assessment. *PLoS ONE* 10:e0118571. <https://doi.org/10.1371/journal.pone.0118571>
- Obligis E, Desportes C, Eymard L, Fernandes ML, Lázaro C, Nunes AL (2011) Tropospheric corrections for coastal altimetry. In: Vignudelli S, Kostianoy A, Cipollini P, Benveniste J (eds) *Coastal altimetry*. Springer, Berlin, pp 147–176. https://doi.org/10.1007/978-3-642-12796-0_6
- Pairaud IL, Lyard F, Auclair F, Letellier T, Marsaleix P (2008) Dynamics of the semi-diurnal and quarter-diurnal internal tides in the Bay of Biscay. Part 1: barotropic tides. *Cont Shelf Res* 28(10):1294–1315. <https://doi.org/10.1016/j.csr.2008.03.004>
- Passaro M, Cipollini P, Vignudelli S, Quartly GD, Snaith HM (2014) ALES: a multi-mission adaptive subwaveform retracker for coastal and open ocean altimetry. *Remote Sens Environ* 145:173–189. <https://doi.org/10.1016/j.rse.2014.02.008>
- Passaro M, Cipollini P, Benveniste J (2015) Annual sea level variability of the coastal ocean: the Baltic Sea-North Sea transition zone. *J Geophys Res Oceans* 120(4):3061–3078. <https://doi.org/10.1002/2014JC010510>
- Passaro M, Dinardo S, Quartly GD, Snaith HM, Benveniste J, Cipollini P, Lucas B (2016). Cross-calibrating ALES Envisat and CryoSat-2 Delay-Doppler: a coastal altimetry study in the Indonesian Seas. *Adv Space Res* 58(3):289–303
- Passaro M, Nadzir ZA, Quartly GD (2018) Improving the precision of sea level data from satellite altimetry with high-frequency and regional sea state bias corrections. *Remote Sens Environ* 18:245–254. <https://doi.org/10.1016/j.rse.2018.09.007>
- Peng F, Deng X (2018) Validation of improved significant wave heights from the Brown-Peaky (BP) retracker along the east coast of Australia. *Remote Sens* 10(7):1072. <https://doi.org/10.3390/rs10071072>

- Piccioni G, Dettmering D, Passaro M, Schwatke C, Bosch W, Seitz F (2018) Coastal improvements for tide models: the impact of ALES retracker. *Remote Sens* 10(5):700
- Piecuch CG, Bittermann K, Kemp AC, Ponte RM, Little CM, Engelhart SE, Lentz SJ (2018) River-discharge effects on United States Atlantic and Gulf coast sea-level changes. *Proc Natl Acad Sci*. <https://doi.org/10.1073/pnas.1805428115>
- Pires N, Fernandes MJ, Gommenginger C, Scharroo R (2016) A conceptually simple modeling approach for Jason-1 sea state bias correction based on 3 parameters exclusively derived from altimetric information. *Remote Sens* 8(7):576. <https://doi.org/10.3390/rs8070576>
- Pires N, Fernandes MJ, Gommenginger C, Scharroo R (2018) Improved sea state bias estimation for altimeter reference missions with altimeter-only three-parameter models. *IEEE Trans Geosci Remote Sens* 99:1–15. <https://doi.org/10.1109/TGRS.2018.2866773>
- Ponte R, Carson M, Cirano M, Domingues C, Jevrejeva S, Marcos M, Mitchum G, Van de Wal RSW, Woodworth PL, Ablain M, Arduin F, Ballu V, Becker M, Benveniste J, Birol F, Bradshaw E, Cazenave A, Demey-Fremaux P, Durand F, Ezer T, Fu LL, Fukumori I, Gordon K, Gravelle M, Griffies SM, Han W, Hibbert A, Hughes CW, Ider D, Kourafalou VH, Little CM, Matthews A, Melet A, Merrifield M, Meyssignac B, Minobe S, Penduff T, Picot N, Piecuch C, Ray RD, Richards L, Santamaria-Gómez A, Stammer D, Staneva J, Testut L, Thompson K, Thompson P, Vignudelli S, Williams J, Williams SDP, Wöppelmann G, Zanna L, Zhang X (2019) Towards comprehensive observing and modeling systems for monitoring and predicting regional to coastal sea level. *OceanObs'19 community white paper*. *Front Mar Sci J Spec Sect Coast Ocean Process*. <https://doi.org/10.3389/fmars.2019.00437>
- Pujol MI, Schaeffer P, Faugère Y, Raynal M, Dibarboure G, Picot N (2018) Gauging the improvement of recent mean sea surface models: a new approach for identifying and quantifying their errors. *J Geophys Res Oceans* 123(8):5889–5911. <https://doi.org/10.1029/2017JC013503>
- Qiu B, Chen S, Klein P, Wang J, Fu L-L, Menemenlis D (2018) Seasonality in transition scale from balanced to unbalanced motions in the world ocean. *J Phys Oceanogr* 48:591–605. <https://doi.org/10.1175/JPO-D-17-0169.1>
- Quarty GD (2010) Hyperbolic retracker: removing bright target artefacts from altimetric waveform data. In: *Proceedings of living planet symposium 2010*, Bergen, Norway, 28 June–2 July 2007, ESA SP-686, ESA Publication, SP-686
- Ray RD, Egbert GD (2017) Tides and satellite altimetry. In situ observations needed to complement, validate, and interpret satellite altimetry. In: Stammer D, Cazenave A (eds) *Satellite altimetry over oceans and land surfaces*. CRC Press, Boca Raton, FL, pp 427–458
- Ray RD, Egbert GD, Erofeeva SY (2011) Tide predictions in shelf and coastal waters: status and prospects. In: Vignudelli S, Kostianoy AG, Cipollini P, Benveniste J (eds) *Coastal altimetry*. Springer, Berlin, pp 191–216. https://doi.org/10.1007/978-3-642-12796-0_8
- Raynal M, Labroue S, Moreau T, Boy F, Picot N (2018) From conventional to Delay Doppler altimetry: a demonstration of continuity and improvements with the Cryosat-2 mission. *Adv Space Res* 62(6):1564–1575. <https://doi.org/10.1016/j.asr.2018.01.006>
- Restano M, Passaro M, Benveniste J (2018) New achievements in coastal altimetry. *Eos*. <https://doi.org/10.1029/2018EO106087>
- Roblou L, Lamouroux J, Bouffard J, Lyard F, Le Hénaff M, Lombard A, Marsaleix P, De Mey P, Birol F (2011) Post-processing altimeter data towards coastal applications and integration into coastal models. In: Vignudelli S, Kostianoy AG, Cipollini P, Benveniste J (eds) *Coastal altimetry*. Springer, Berlin, pp 217–246. https://doi.org/10.1007/978-3-642-12796-0_9
- Roca M, Laxon S, Zeli C (2009) The EnviSat-RA2 instrument design and tracking performance. *IEEE Trans Geosci Remote Sens* 47:3489–3506. <https://doi.org/10.1109/TGRS.2009.2020793>
- Rodríguez E (2016) Surface water and ocean topography mission project. Science requirements doc., revision A. California Institute of Technology Jet Propulsion Laboratory Publ. JPL D-61923
- Roemmich D, Woodworth P, Jevrejeva S, Purkey S, Lankhorst M, Send U, Nikolai Maximenko N (2017) In situ observations needed to complement, validate, and interpret satellite altimetry. In: Stammer D, Cazenave A (eds) *Satellite altimetry over oceans and land surfaces*. CRC Press, Boca Raton, FL, pp 113–147
- Roscher R, Uebbing B, Kusche J (2017) STAR: spatio-temporal altimeter waveform retracking using sparse representation and conditional random fields. *Remote Sens Environ* 201:148–164. <https://doi.org/10.1016/j.rse.2017.07.024>
- Scharroo R, Leuliette EW, Lillibridge JL, Byrne D, Naeije MC, Mitchum GT (2013) RADS: consistent multi-mission products. In: *Proceedings of 20 years of progress in radar altimetry symposium*, Venice, Italy, 24–29 September 2012, ESA SP-710. <https://doi.org/10.5270/esa.sp-710.altimetry2012>

- Stammer D, Cazenave A (2017) Satellite altimetry over oceans and land surfaces. CRC Press, Boca Raton, FL, p 670
- Stammer D, Ray RD, Andersen OB, Arbic BK, Bosch W, Carrère L, Cheng Y, Chinn DS, Dushaw BD, Egbert GD, Erofeeva SY, Fok HS, Green JAM, Griffiths S, King MA, Lapin V, Lemoine FG, Lutiche SB, Lyard F, Morison J, Müller M, Padman L, Richman JG, Shriver JF, Shum CK, Taguchi E, Yi Y (2014) Accuracy assessment of global barotropic ocean tide models. *Rev Geophys* 52(3):243–282. <https://doi.org/10.1002/2014RG000450>
- Toublanc F, Ayoub NK, Lyard F, Marsaleix P, Allain DJ (2018) Tidal downscaling from the open ocean to the coast: a new approach applied to the Bay of Biscay. *Ocean Model* 124:16–32. <https://doi.org/10.1016/j.ocemod.2018.02.001>
- Tran N, Vandemark D, Chapron B, Labroue S, Feng H, Beckley B, Vincent P (2006) New models for satellite altimeter sea state bias correction developed using global wave model data. *J Geophys Res* 111:C09009. <https://doi.org/10.1029/2005JC003406>
- Tran N, Labroue S, Philipps S, Bronner E, Picot N (2010) Overview and update of the sea state bias corrections for the Jason-2, Jason-1 and TOPEX missions. *Mar Geod* 33:348. <https://doi.org/10.1080/01490419.2010.487788>
- Troupin C, Pascual A, Valladeau G, Pujol I, Lana A, Heslop E, Ruiz S, Torner M, Picot N, Tintoré J (2015) Illustration of the emerging capabilities of SARAL/AltiKa in the coastal zone using a multi-platform approach. *Adv Space Res* 55(1):51–59. <https://doi.org/10.1016/j.asr.2014.09.011>
- Valladeau G, Thibaut P, Picard B, Poisson JC, Tran N, Picot N, Guillot A (2015) Using SARAL/AltiKa to improve Ka-band altimeter measurements for coastal zones, hydrology and ice: the PEACHI prototype. *Mar Geod* 38(sup1):124–142. <https://doi.org/10.1080/01490419.2015.1020176>
- Verron J, Bonnefond P, Aouf L, Birol F, Bhowmick SA, Calmant S, Conchy T, Crétaux J-F, Dibarbouré G, Dubey AK, Faugère Y, Guerreiro K, Gupta PK, Hamon M, Jebri F, Kumar R, Morrow R, Pascual A, Pujol M-I, Rémy E, Rémy F, Smith WHF, Tournadre J, Vergara O (2018) The benefits of the Ka-band as evidenced from the SARAL/AltiKa altimetric mission: scientific applications. *Remote Sens* 10:163. <https://doi.org/10.3390/rs10020163>
- Vieira T, Fernandes MJ, Lázaro C (2018) Independent assessment of on-board microwave radiometer measurements in coastal zones using tropospheric delays from GNSS. *IEEE Trans Geosci Remote Sens*. <https://doi.org/10.1109/TGRS.2018.2869258>
- Vignudelli S, Cipollini P, Roblou L, Lyard F, Gasparini GP, Manzella G, Astraldi M (2005) Improved satellite altimetry in coastal systems: case study of the Corsica Channel (Mediterranean Sea). *Geophys Res Lett* 32:L07608. <https://doi.org/10.1029/2005GL022602>
- Vignudelli S, Snaith HM, Lyard F, Cipollini P, Birol F, Bouffard J, Roblou L (2006) Satellite radar altimetry from open ocean to coasts: challenges and perspectives. In: Proceedings of 5th Society of Photo-Optical Instrumentation Engineers (SPIE) Asia-Pacific remote sensing symposium, Panaji, Goa, India, 13–17 November 2006, 6406, 64060L, pp 1–12. <https://doi.org/10.1117/12.694024>
- Vignudelli S, Vignudelli S, Kostianoy AG, Cipollini P, Benveniste J (eds) (2011a) Coastal altimetry. Springer, Berlin. <https://doi.org/10.1007/978-3-642-12796-0>
- Vignudelli S, Cipollini P, Gommenginger C, Snaith H, Coelho H, Fernandes J, Lázaro C, Nunes A, Gómez-Enri J, Martín-Puig C, Woodworth P, Dinardo S, Benveniste J (2011b) Satellite altimetry: sailing closer to the coast. In: Gower J, Levy G, Heron M, Tang D, Katsaros K, Singh R (eds) Remote sensing of the changing oceans. Springer, Berlin, pp 217–238. https://doi.org/10.1007/978-3-642-16541-2_11
- Vignudelli S, De Basio F, Scozzari A, Zecchetto S, Papa A (2019) Sea level trends and variability in the Adriatic Sea and around Venice. In: Proceedings of international association of geodesy symposia—international review workshop on satellite altimetry Cal/Val activities and applications, 23–26 April 2018, Crete, Greece, 1–10, Springer, Berlin. https://doi.org/10.1007/1345_2018_51
- Vu PL, Frappart F, Darrozes J, Marieu V, Blarel F, Ramillien G, Bonnefond P, Birol F (2018) Multi-satellite altimeter validation along the French Atlantic Coast in the Southern Bay of Biscay from ERS-2 to SARAL. *Remote Sens* 10(1):93. <https://doi.org/10.3390/rs10010093>
- Wang J, Fu LL, Torres HG, Chen S, Qiu B, Menemenlis D (2019) On the spatial scale to be resolved by the surface water and ocean topography Ka-band fadar interferometer. *J Atmos Ocean Technol* 36(1):87–99. <https://doi.org/10.1175/JTECH-D-18-0119.1>
- Woodworth PL, Hunter JR, Marcos M, Caldwell P, Menéndez M, Haigh I (2016) Towards a global higher-frequency sea level dataset. *Geosci Data J* 3(2):50–59. <https://doi.org/10.5285/3b602f74-8374-1e90-e053-6c86abc08d39>
- Woodworth PL, Wöppelmann G, Marcos M, Gravelle M, Bingley RM (2017) Why we must tie satellite positioning to tide gauge data. *Eos* 98(4):13–15. <https://doi.org/10.1029/2017EO064037>

- Wright LD, Nichols CR (2018) Tomorrow's coasts: complex and impermanent, vol 27. Coastal research library. Springer, Berlin. <https://doi.org/10.1007/978-3-319-75453-6>
- Wright LD, Syvitski JPM, Nichols CR (2018) Sea level rise: recent trends and future projections. In: Wright LD, Nichols CR (eds) Tomorrow's coasts: complex and impermanent. Springer, Berlin. <https://doi.org/10.1007/978-3-319-75453-6>
- Xu XY, Birol F, Cazenave A (2018) Evaluation of coastal sea level offshore Hong Kong from Jason-2 altimetry. *Remote Sens* 10(2):282. <https://doi.org/10.3390/rs10020282>
- Yang Y, Hwang C, Hsu HJ, Dongchen E, Wang H (2011) A subwaveform threshold retracker for ERS-1 altimetry: a case study in the Antarctic Ocean. *Comput Geosci* 41:88–98. <https://doi.org/10.1016/j.cageo.2011.08.017>
- Yang L, Lin M, Liu Q, Pan D (2012) A coastal altimetry retracking strategy based on waveform classification and sub-waveform extraction. *Int J Remote Sens* 33(24):7806–7819. <https://doi.org/10.1080/01431161.2012.701350>

Publisher's Note Springer Nature remains neutral with regard to jurisdictional claims in published maps and institutional affiliations.

Affiliations

Stefano Vignudelli¹ · Florence Birol² · Jérôme Benveniste³ · Lee-Lueng Fu⁴ · Nicolas Picot⁵ · Matthias Raynal⁶ · Hélène Roinard⁶

Florence Birol
florence.birol@legos.obs-mip.fr

Jérôme Benveniste
Jerome.Benveniste@esa.int

Lee-Lueng Fu
llf@jpl.nasa.gov

Nicolas Picot
nicolas.picot@cnes.fr

Matthias Raynal
mraynal@cls.fr

Hélène Roinard
hroinard@cls.fr

¹ Consiglio Nazionale delle Ricerche (CNR-IBF), Via Moruzzi 1, 56127 Pisa, Italy

² Laboratoire d'Etudes en Géophysique et Océanographie Spatiales (LEGOS), 18, av. Edouard Belin, 31401 cédex 9 Toulouse, France

³ European Space Agency (ESA-ESRIN), Largo Galileo Galilei, 1, 00044 Frascati, Rome, Italy

⁴ Jet Propulsion Laboratory (JPL), National Aeronautics and Space Administration (NASA), 4800 Oak Grove Dr, Pasadena, CA 91109, USA

⁵ Centre National d'Études Spatiales (CNES), 18 Avenue Edouard Belin, 31400 Toulouse, France

⁶ Collecte Localisation Satellites (CLS), 11 Rue Hermès 31520 Ramonville-Saint-Agne, France